Molecular Pharmacology Fast Forward. Published on May 17, 2006 as doi: 10.1124/mol.105.021600
This article has not been copyedited and formatted. The final version may differ from this version.

MOLPHARM/2005/021600

TGFβR1 kinase activity, but not p38 activation is required for TGFβR1-induced myofibroblast differentiation and pro-fibrotic gene expression

Ann M. Kapoun, Nicholas J. Gaspar*, Ying Wang*, Debby Damm, Yu-Wang Liu, Gilbert O'Young, Diana Quon, Andrew Lam, Kimberly Munson, Thomas-Toan Tran, Jing Ying Ma, Alison Murphy, Sundeep Dugar, Sarvajit Chakravarty, Andrew A. Protter, Fu-Qiang Wen, Xiangde Liu, Stephen I. Rennard, and Linda Slanec Higgins

Scios Inc. Fremont, California: AMK, NJG, YW, DD, YL, GO, DQ, AL, KM, TT, JYM, AP, LSH, AM, SD, SC

Nebraska Medical Center, Omaha, Nebraska: FW, XL, SIR

*Both authors contributed equally to this work

Molecular Pharmacology Fast Forward. Published on May 17, 2006 as DOI: 10.1124/mol.105.021600
This article has not been copyedited and formatted. The final version may differ from this version.

MOLPHARM/2005/021600

Running Title: TGFβR1 and p38 signaling in human lung fibroblasts

Address correspondence to: Ann M. Kapoun, Ph.D., 6500 Paseo Padre Parkway, Fremont, CA 94555. E-mail:kapoun@sciosinc.com, Telephone 510.739.2250, Telefax 510.739.4545

Number of total pages=46

Number of tables= 3

Number of figures= 10

Number of references= 45

Number of words in Abstract= 214

Number of words in Introduction= 465

Number of words in Discussion= 1415

Non-standard abbreviations.

SMAD, mothers against DPP homolog; TGFβ, Transforming growth factor-β; ECM, extracellular matrix; MAPK, p38 mitogen-activated kinase; HLF, human lung fibroblast

Molecular Pharmacology Fast Forward. Published on May 17, 2006 as DOI: 10.1124/mol.105.021600
This article has not been copyedited and formatted. The final version may differ from this version.

Abstract.

Transforming growth factor-β (TGFβ) is a major mediator of normal wound healing and of pathological conditions involving fibrosis such as idiopathic pulmonary fibrosis. TGFβ also stimulates the differentiation of myofibroblasts, a hallmark of fibrotic diseases. Here, we examined the underlying processes of TGFβR1 kinase activity in myofibroblast conversion of human lung fibroblasts using specific inhibitors of TGFβR1 (SD-208) and p38 mitogen-activated kinase (SD-282). We demonstrated that SD-208, but not SD-282, inhibited TGFβ-induced: SMAD signaling, myofibroblast transformation, and collagen gel contraction. Furthermore, we extended our findings to a rat bleomycin-induced lung fibrosis model, demonstrating a significant decrease in the number of myofibroblasts at fibroblastic foci in SD-208, but not SD-282 treated animals. SD-208 also reduced collagen deposition in this *in vivo* model. Microarray analysis of human lung fibroblasts identified molecular fingerprints of these processes, and showed that SD-208 had global effects on reversing TGFβ-induced genes involved in fibrosis, inflammation, cell proliferation, cytoskeletal organization, and apoptosis. These studies also revealed that while the p38 pathway may not be needed for appearance or disappearance of the myofibroblast, it can mediate a subset of inflammatory and fibrogenic events of the myofibroblast during the process of tissue repair and fibrosis. Our findings suggest that inhibitors such as SD-208 may be therapeutically useful in human interstitial lung diseases and pulmonary fibrosis.

Molecular Pharmacology Fast Forward. Published on May 17, 2006 as DOI: 10.1124/mol.105.021600
This article has not been copyedited and formatted. The final version may differ from this version.

Introduction.

Pulmonary fibrosis is a pathological hallmark of interstitial lung diseases (Green, 2002). A common feature of fibrosis is the increased deposition of the extracellular matrix (ECM). Myofibroblasts are instrumental in fibrogenic processes in pulmonary fibrosis, as they are the major producers of ECM proteins. Commonly identified by the expression of α-smooth muscle actin, myofibroblasts are considered to be an intermediate between a fibroblast and a true smooth muscle cell. As such, they are involved in wound healing and contraction. There are substantial data showing the presence of myofibroblasts in lung tissues from patients with pulmonary fibrosis (Phan, 2002).

TGFβ, a major player in the conversion of fibroblasts to myofibroblasts, is a pleiotropic growth factor involved in multiple biological processes including cell proliferation, fibrosis, tissue repair, inflammation, apoptosis, cell differentiation, cell adhesion, and motility (Grande, 1997; Massague et al., 1994; Sporn and Roberts, 1992). TGFβ levels are elevated in the bronchoalveolar lavage fluid in patients with pulmonary fibrosis (Kuroki et al., 1995; Ludwicka et al., 1995) and in the lungs of animals with experimentally induced lung fibrosis (Coker et al., 1997). TGFβ signals through heteromeric receptor complexes consisting of type I (TGFβR1) and type II (TGFβR11) serine-threonine kinase receptors. Upon ligand binding, TGFβR11 transphosphorylates TGFβR1. The activated receptor then phosphorylates and activates members of the SMAD family of proteins. Receptor SMADs subsequently bind to co-SMAD4 and

Molecular Pharmacology Fast Forward. Published on May 17, 2006 as DOI: 10.1124/mol.105.021600
This article has not been copyedited and formatted. The final version may differ from this version.

translocate into the nucleus where they regulate the transcriptional response of target genes.

Besides signaling through SMADs, several additional pathways have also been shown to mediate the downstream signaling from TGFβR1. These include the p38 mitogen-activated kinase (MAPK) (Bakin et al., 2002; Bhowmick et al., 2001), the c-Jun NH_2-terminal kinase (JNK) (Atfi et al., 1997), the extracellular-regulated kinase (ERK) (Frey and Mulder, 1997), and the phosphatidylinositol kinase (PI3K) pathways (Bakin et al., 2000). The p38 pathway is involved in a variety of biological responses to the TGFβ signaling such as migration of smooth muscle cells (Hedges et al., 1999), neuronal differentiation of PC12 cells (Iwasaki et al., 1999), chondrogenesis of ATDC-5 cells (Nakamura et al., 1999) and cardiomyocyte differentiation (Monzen et al., 1999). Despite the numerous implications of p38 signaling in the TGFβ pathway, the significance of TGFβ-mediated p38 signaling in pulmonary fibrosis and myofibroblast transformation is not well defined.

Here, we used a combination of cDNA arrays and small molecule inhibitors of TGFβ-R1 and p38 MAP kinase to begin to delineate the molecular events downstream of TGFβ-R1. We identify a number of TGFβ-regulated genes and assess which genes are regulated by p38. Also, we show that small molecule inhibitors of TGFβR1, but not p38, block SMAD signaling, inhibit an *in vitro* model of fibrotic tissue remodeling—fibroblast

Molecular Pharmacology Fast Forward. Published on May 17, 2006 as DOI: 10.1124/mol.105.021600
This article has not been copyedited and formatted. The final version may differ from this version.

mediated collagen gel contraction, and prevent the transformation of fibroblasts to myofibroblasts *in vivo* and *in vitro*, as measured by expression of α-smooth muscle actin.

Molecular Pharmacology Fast Forward. Published on May 17, 2006 as DOI: 10.1124/mol.105.021600
This article has not been copyedited and formatted. The final version may differ from this version.

Materials and Methods.

Cell Culture and Inhibitor Reagents

Three lots of primary human lung fibroblast (HLF) cells, derived from a 40 year old female (donor A, Lot 8F162), a 10 year old male (donor B, Lot 17423), and a 51 year old female (donor C, Lot 4F0512), were provided by Cambrex Bio Science (Walkersville, Md). Real-time RT-PCR experiments were performed on samples from all donors. The microarray and gel contraction experiments were performed on cells from donor A, and the ELISA and Westerns data were assayed using samples from donors A and C. Cells were seeded at $4x10^5$ cells (passage 4) in 100 mm^2 dishes and cultured in complete FGM (fibroblast growth medium, Cambrex Bio Science). The next day, medium was changed to FGM without serum or fibroblast growth factor, but supplemented with 0.2% bovine serum albumin and 50 µg/mL vitamin C. Cells for real-time RT-PCR and microarray serum were deprived for 24 h prior to treating with 5 ng/mL TGFβ1 (R&D Systems, Minneapolis, MN) in the presence or absence of 400 nmol/L SD-208 or 400 nmol/L SD-282. Concentrations of inhibitors were chosen based on IC_{50s} in HLF cell-based assays (data not shown and Figure 2, IC_{50} 70-80 nmol/L). Induction with TGFβ was carried out for various times (7.5 h, 24 h, and 72 h) after which RNA was harvested by lysing the cells in RLT™ buffer (Qiagen, Valencia, CA) and frozen at -80°C.

Molecular Pharmacology Fast Forward. Published on May 17, 2006 as DOI: 10.1124/mol.105.021600
This article has not been copyedited and formatted. The final version may differ from this version.

SD-208 and SD-282 kinase assays

TGFβR1 kinase inhibitor SD-208 and p38α MAP kinase inhibitor SD-282 were synthesized by the Medicinal Chemistry Department at Scios, Inc. and dissolved in DMSO. They were designed from medicinal chemistry efforts optimizing high-throughput screening leads into potent, selective inhibitors with acceptable pharmaceutical properties. SD-282 is an indole-5-carboxamide, ATP competitive inhibitor of p38α MAP kinase and SD-208 is a 2,4-disubstituted pteridine, ATP competitive, inhibitor of TGFβR1 kinase (Figure 1). SD-282 was prepared by functionalizing the 3-position of the corresponding indole-5-carboxamide through treatment with oxalyl chloride in methylene chloride followed by addition of dimethylamine. The resulting material was purified by silica gel chromatography and then converted to its hydrochloride salt form. SD-208 was prepared by heating 4-chloro-2-(5-chloro-2-fluorophenyl)pteridine with 4-aminopyridine and triethylamine in DMF. The resulting material was purified by silica gel chromatography and then converted to its hydrochloride salt form.

Kinase assays were performed by standard methods (Davies et al., 2000). Briefly, kinases were assayed by measuring the incorporation of radiolabeled ATP into a peptide or protein substrate. Reactions were performed in 96-well plates and included the relevant kinase, substrate, ATP, and appropriate co-factors. The reactions were incubated and then stopped by the addition of phosphoric acid. Substrate was captured onto a phosphocellulose filter, which was washed free of unreacted γ-^{33}P-ATP from Perkin

Elmer Life Sciences. The counts incorporated were determined by counting on a microplate scintillation counter (TopCount, Perkin Elmer Corporation, Boston, MA). The ability of compounds to inhibit the kinase was determined by comparing the counts incorporated in the presence of compound to those in the absence of compound.

Western Blot and ELISA Analysis

HLF cells were serum-starved for 24 h in FGM medium (Cambrex, Walkersville, MD) containing no serum or FGF but supplemented with 0.2% BSA and 50 μg/mL vitamin C. To analyze SMAD phosphorylation, cells were treated with 2 ng/mL TGFβ1 for 30 minutes in the presence of increasing concentrations of SD-208 or SD-282 inhibitor as indicated. To analyze induction of α-smooth muscle actin, CTGF, and PAI-1, cells were treated with 2 ng/mL TGFβ1 for 7, 24 or 72 h in the presence of 400 nmol/L SD-208 or SD-282. Total cell lysates were prepared in MPER buffer (mammalian protein extraction reagent**,** Pierce, Rockford, IL) or in RIPA (10 nmol/L Tris pH 8.0, 150 mmol/L NaCl, 1% Triton X-100, 1% deoxycholate, and 0.1% SDS, Roche, Indianapolis, IN) containing protease and phosphatase inhibitor cocktails. Aliquots of the cell lysates were fractionated on SDS-polyacrylamide gels and transferred to nitrocellulose membranes (Invitrogen Life Technologies, Carlsbad, CA). The membranes were blocked against nonspecific binding using 4% skim milk. Proteins were detected using specific primary antibodies and peroxidase-conjugated secondary antibodies. The antibody against phospho-SMAD2 was from Cell Signaling Technology (Beverly, MA); the mouse

Molecular Pharmacology Fast Forward. Published on May 17, 2006 as DOI: 10.1124/mol.105.021600
This article has not been copyedited and formatted. The final version may differ from this version.

monoclonal antibody against SMAD2 was purchased from BD Biosciences (Palo Alto, CA); the CTGF polyclonal antibody was custom made (U. Schellenberger, Scios Inc); the monoclonal antibody against α-smooth muscle actin was purchased from Sigma (St. Louis, MO); the mouse monoclonal antibody against GAPDH was from Biogenesis (UK); and the mouse monoclonal antibody against vimentin was from Affinity Bioreagents (Golden, CO). The blots were visualized by the SuperSignal West Femto™ detection system (Pierce) or the Amersham ECL detection system followed by quantitation using Image Quant 5.2 (Amersham Biosciences Corp, Piscataway, NJ).

Phospho-SMAD ELISA assays were performed in 96-well plates coated with anti-SMAD2/3 monoclonal antibodies (BD Biosciences, 100 ng/well) for 18 h at 4°C or 2 h at room temperature. To block non-specific binding, excess antibody was removed and the wells were treated with blocking buffer (0.3% BSA/PBS) for 2 h at room temperature. The wells were rinsed 3 times with wash buffer (0.5% Tween-20/PBS), and cell lysates (10 ug total protein) were added to each well and incubated overnight at 4°C. Wells were rinsed 3 times with wash buffer before adding a polyclonal anti-phospho-SMAD2/3 antisera diluted in 2% BSA/0.5% Tween-20/PBS. Following a 2 h incubation at room temperature, wells were washed 3 times with wash buffer before developing with tetramethyl benzidine (TMB, Sigma). Reactions were stopped with 0.5 N H_2SO_4 after a 5-30 min incubation, and plates were read at OD450 in a SpectraMax 250 plate reader (Molecular Devices, Sunnyvale, CA). For PAI-1 ELISA analysis, Imulyse (Biopool International, Ventura, CA) kits were used according to manufacturers instructions.

Molecular Pharmacology Fast Forward. Published on May 17, 2006 as DOI: 10.1124/mol.105.021600
This article has not been copyedited and formatted. The final version may differ from this version.

In vitro Immunofluorescence Analysis

To examine the TGFβ-induced nuclear translocation of SMAD2, HLF cells were grown to 50-80% confluence in Lab-Tek™ Chamber Slides (Nalge Nunc International, Naperville, IL). Cells were serum starved and treated with TGFβ1 (2 ng/mL) and inhibitors as described above. After treatment, cells were washed with PBS and fixed for 15 minutes with 4% paraformaldehyde in PBS. Cells were then treated with 0.1% saponin in PBS for 10 minutes. After washing off the detergent, fixed cells were incubated with primary antibodies overnight at 4°C. Specific antibodies for SMAD2 were from Zymed Laboratories (South San Francisco, CA). After extensive washing, the biotinylated anti-rabbit IgG and fluorescein avidin D secondary antibodies (Vector Laboratories, Burlingame, CA) were added. The fluorescence images of SMAD2 were visualized by a Nikon™ microscope using Image-pro plus 4.5™ software.

Collagen Gel Contraction

Native type I collagen (Rat Tail Tendon Collagen, RTTC) was extracted from rat tail tendons by a previously published method (Bell et al., 1979; Mio et al., 1996). Briefly, tendons were excised from rat tails without tendon sheath and other connective tissues. Repeated washing with Tris -buffered saline was followed by dehydration and sterilization with 50%, 75%, 95% and pure ethanol. Type I collagen was then extracted in 6 mmol/L hydrochloric acid at 4°C. The supernatant was harvested by centrifugation at

Molecular Pharmacology Fast Forward. Published on May 17, 2006 as DOI: 10.1124/mol.105.021600
This article has not been copyedited and formatted. The final version may differ from this version.

3000 g for 1 h at 4°C. Collagen concentration was determined by weighing a lyophilized aliquot from each lot of collagen solution.

Gels were prepared using a previously described method (Mio et al., 1996; Mio et al., 1998) by mixing RTTC, distilled water, and 4-times concentrated Dulbecco's Modified Eagle Medium (DMEM) so that the final mixture resulted in a physiologic ionic strength, 1 x DMEM and a pH of 7.40. Cells were trypsinized (Trypsin-EDTA; 0.05% trypsin, 0.53 mmol/L EDTA-4Na, GIBCO™ Invitrogen Life Technologies, Carlsbad, CA) and suspended in 10 mL complete FGM medium and counted with Coulter Counter. HLF cells were pelleted and resuspended in basal FGM without serum or other growth factors at a density of 10^7 cells/mL. Cells were then mixed with the neutralized collagen solution so that the final cell density in the collagen solution was $5x10^5$ cells/mL, and the final concentration of collagen was 0.75 mg/mL. Aliquots (0.5 mL/well) of the mixture of cells in collagen were cast into each well of 24-well tissue culture plates (BD Biosciences). After gelation was completed within 20 minutes at room temperature, the gels were gently released from the 24 well tissue culture plates and transferred into 60 mm tissue culture dishes (3 gels in each dish), which contained 5 mL of freshly prepared basal FGM medium with or without TGF-β1 (200 pmol/L) or inhibitors. The gels were then incubated at 37°C in a 5% CO_2 atmosphere for 2 days and the area of each gel was measured with an Optomax V image analyzer (Optomax, Burlington, MA) daily. Data were expressed as the percentage of area compared to the original gel size.

Molecular Pharmacology Fast Forward. Published on May 17, 2006 as DOI: 10.1124/mol.105.021600
This article has not been copyedited and formatted. The final version may differ from this version.

Histology and Immunohistochemistry in the Rat Bleomycin Model

Sprague-Dawley rats were administered bleomycin for 14 days. Rats were intubated and aerosolized with 200 μL of saline or 1.0 unit of bleomycin per rat (3 to 4 rats per group). One day following bleomycin challenge rats were treated twice daily with vehicle or vehicle plus SD-208 (60 mg/kg in 1% methyl cellulose) or SD-282 (60 mg/kg in 1% PEG-400). Inhibitor doses were chosen based on efficacious doses from our previous studies (Bonniaud et al., 2005; Li et al., 2004). Also, the inhibitor doses used in this study have been shown to have pharmacological effects in the lungs of bleomycin challenged rats as demonstrated by the inhibition of *CTGF* mRNA by SD-208 and of *COX2* mRNA by SD-282 (data not shown). Lungs were removed en bloc; they were inflated with 4% formalin at a constant pressure of 15 cm of water and then fixed in 10% formalin for 48 h. The left lung was cut perpendicular to the tracheobronchial tree into sections. Tissue sections were processed, paraffin embedded, cut 5 μm thick, and immunohistochemistry stained using mouse antibodies against α-smooth muscle actin (Chemicon International, Inc, Temecula, CA). Negative control sections were run in parallel with normal mouse IgG2α diluted to the same concentration as the primary antibody (data not shown). The number of myofibroblasts was measured under the Nikon E600™ light microscope equipped with a Spot™ digital camera at magnification of X400 for 36-40 fields (for each animal). Positively stained smooth muscle cells surrounding major airways and blood vessels were excluded from the analysis.

Molecular Pharmacology Fast Forward. Published on May 17, 2006 as DOI: 10.1124/mol.105.021600
This article has not been copyedited and formatted. The final version may differ from this version.

Measurement of Hydroxyproline Content

To quantify lung collagen content as an indicator of pulmonary fibrosis, the hydroxyproline content in whole lungs was measured in all animals (7 to 8 animals per group) according to published methods (Woessner, 1961). Briefly, lung samples were minced into fine pieces with a scissors and homogenized thoroughly in 15 mL of 1X PBS with a Polytron. One mL of whole homogenate was precipitated with 0.25 mL of ice-cold 50% (w/v) trichloroacetic acid. The precipitate was hydrolyzed in 2.0 mL of 6N HCL for 18 h at 110 ^{o}C**.** After neutralization, hydroxyproline content was determined. The results were calculated as μg hydroxyproline per whole lung using hydroxyproline standards from Sigma (St. Louis, MO).

cDNA Microarray

Gene expression profiles were determined from cDNA microarrays as previously described (Kapoun et al., 2004). Briefly, arrays containing 8,600 elements were derived from clones isolated from normalized cDNA libraries or purchased from ResGen (Invitrogen Life Technologies). Clones were sequence verified, and differentially expressed genes were reconfirmed by NCBI BLAST analyses. Differential expression values were expressed as the ratio of the median of background-subtracted fluorescent intensity of the experimental RNA to the median of background-subtracted fluorescent intensity of the control RNA. For ratios greater than or equal to 1.0, the ratio was

Molecular Pharmacology Fast Forward. Published on May 17, 2006 as DOI: 10.1124/mol.105.021600
This article has not been copyedited and formatted. The final version may differ from this version.

expressed as a positive value. For ratios less than 1.0, the ratio was expressed as the negative reciprocal (e. g., a ratio of 0.5 = -2.0). Differential expression ratios were determined as the mean of the two values from dye-swapped duplicates. Expression data was rejected if neither channel produced a signal of at least 2.0-fold over background. Statistically significant differential expression threshold values were determined according to the method of Yang *et al* (Yang et al., 2002). Hierarchical clustering was used to visualize the data and to group genes into similar expression patterns (Spotfire, Somerville, MA). The data were prepared for clustering by using the log base 10 of the median expression values and then normalized by the Z-score method within Spotfire.

mRNA Isolation, Labeling, and Hybridizations

Total RNA was extracted from cells using Qiagen's RNeasy™ kit. RNA was amplified using a modified Eberwine protocol (Kapoun et al., 2004) that incorporated a polyA tail into the amplified RNA. Fluorescently-labeled cDNA probes were generated by reverse transcription of 4 μg of RNA with SuperScript II™ (Invitrogen Life Technologies) using anchored dT primers in the presence of Cy3 or Cy5 dUTP as previously described (Kapoun et al., 2004). Hybridization of each fluorophore was quantified using an Axon GenePix 4000A™ scanner.

Molecular Pharmacology Fast Forward. Published on May 17, 2006 as DOI: 10.1124/mol.105.021600
This article has not been copyedited and formatted. The final version may differ from this version.

Real-time RT-PCR

Real-time RT-PCR was performed in a two-step manner. cDNA synthesis and real-time detection were carried out in a PTC-100™ Thermal Cycler (MJ Research Inc, Waltham, MA) and an ABI Prism™ 7900 Sequence Detection System (Applied Biosystems, Foster City, CA), respectively. Random hexamers (Qiagen, Valencia, CA) were used to generate cDNA from 200 ng RNA as described in Applied Biosystems User Bulletin #2. TaqMan™ PCR Core Reagent Kit or TaqMan™ Universal PCR Master Mix (Applied Biosystems) were used in subsequent PCR reactions according to the manufacturer's protocols. Relative quantitation of gene expression was performed using the relative standard curve method.

Sequence specific primers and probes were designed using Primer Express Version 2™ software (Applied Biosystems). Sequences of primers and probes can be found in Supplemental Table E1. Expression levels were normalized to 18S rRNA. All real-time RT-PCR reactions were performed in triplicate on each of the 3 biological replicates from each donor.

Statistical Analysis

The experiments were usually performed 3-4 times with similar results. Significance was tested by one or two tailed ANOVA followed by Bonferroni's correction using PRISM4 software (GraphPad Software Inc. San Diego, CA) unless otherwise indicated.

Molecular Pharmacology Fast Forward. Published on May 17, 2006 as DOI: 10.1124/mol.105.021600
This article has not been copyedited and formatted. The final version may differ from this version.

Results

TGFβR1 Kinase Inhibitor, SD-208, Blocks SMAD Signaling in HLF Cells

The initial characterization of SD-208 and SD-282 in cell-free assays led to their identification as a potent inhibitors of TGFβR1 and p38 MAPK. SD-208 has an IC_{50} of 49 nmol/L based on direct enzymatic assay of TGFβR1 kinase activity with specificity of at least >17-fold over members of a panel of related protein kinases (Table 1). SD-282 is a small molecule, ATP-competitive, specific inhibitor of p38α and p38β MAP kinase, and demonstrates 14-fold selectivity for p38α versus p38β MAP kinase (IC_{50} 1.6 nmol/L and 23 nmol/L, respectively, Table 2).

As SMAD phosphorylation and nuclear translocation are well-characterized steps in TGFβ signaling, we tested the ability of pharmacological inhibitors of TGFβR1 kinase and p38 MAPK to modulate these events. HLF cells were treated with TGFβ for 30 minutes in the presence of either a small molecule inhibitor of TGFβR1 (SD-208) or of p38 MAP kinase (SD-282) for 30 minutes.

ELISA and Western blot analysis showed that SD-208, but not SD-282, inhibited TGFβ-induced SMAD2/3 and SMAD2 phosphorylation, respectively, in a dose-dependent manner (0 – 400 nmol/L; Figure 2). In addition, SD-208 blocked TGFβ-induced nuclear translocation of SMAD2 in HLF cells, however SD-282 had no effect (Figure 3). These results show that SD-208 is an effective inhibitor of TGFβ-induced SMAD signaling and suggest that p38 has no direct role in SMAD mediated signaling during myofibroblast differentiation.

Molecular Pharmacology Fast Forward. Published on May 17, 2006 as DOI: 10.1124/mol.105.021600
This article has not been copyedited and formatted. The final version may differ from this version.

TGFβR1 Kinase Inhibitor, SD-208, Inhibits Myofibroblast Differentiation and Collagen Gel Contraction in HLF Cells

To test the functional significance of SD-208 and SD-282, the inhibitors were evaluated for their effects on TGFβ-induced myofibroblast transformation and collagen gel contraction. Protein levels of α-smooth muscle actin expressed by myofibroblasts were measured from HLF cells treated for 24 and 72 h with TGFβ. Treatment with TGFβ resulted in increased levels of α-smooth muscle actin; co-treatment with SD-208 showed a >80 % reduction in α-smooth muscle actin levels when compared to TGFβ treatment alone at 24 and 72 h (Figure 4). In contrast, SD-282 had no significant effect on TGFβ-induced α-smooth muscle actin. Similar effects were also seen in the absence of TGFβ stimulation showing that SD-208 also inhibits basal levels of α-smooth muscle actin.

TGFβ was added to collagen gels containing HLF cells in the presence or absence of SD-208 and SD-282. Treatment of fibroblasts with TGFβ increased the contraction of collagen gels mediated by HLF cells (Figure 5). The addition of SD-208, but not SD-282, significantly inhibited this gel contraction in a dose dependent manner. Together, these data demonstrate that TGFβR1 kinase inhibition and not p38 MAPK inhibition effectively block the fibrogenic properties of TGFβ in human lung fibroblasts.

Molecular Pharmacology Fast Forward. Published on May 17, 2006 as DOI: 10.1124/mol.105.021600
This article has not been copyedited and formatted. The final version may differ from this version.

TGFβR1 Kinase Inhibitor SD-208 Inhibits Myofibroblast Differentiation and collagen deposition *in vivo* in Bleomycin Treated Rat Lungs

We performed α-smooth muscle actin immunohistochemistry in a rodent model of pulmonary fibrosis, to compare our *in vitro* observations of the effects of TGFβR1 and p38 blockades on myofibroblast conversion to an *in vivo* system. Bleomycin induces acute lung injury followed by chronic fibrosis in a dose-dependent manner in both humans and in experimental animals. Here, we tested the effects of SD-208 and SD-282 in a rat model of bleomycin induced fibrosis (Thrall et al., 1979) in which TGFβ is thought to be a critical mediator of pathogenesis. Rats were treated with vehicle, SD-208 (60 mg/kg/orally twice daily), or SD-282 (60 mg/kg/orally twice daily) one day following bleomycin administration and continued for 14 days.

Saline-treated rats stained positive for α-smooth muscle actin around major airways and blood vessels, whereas bleomycin-treated animals had significantly higher numbers of myofibroblasts (α-smooth muscle actin positive cells) at the fibroblastic foci (Figure 6). SD-208, but not SD-282, significantly reduced the number of cells staining positive for α-smooth muscle actin (Figure 6). In a repeat experiment, lung hydroxyproline content was measured in SD-208 treated animals compared to vehicle control (Figure 7). Hydroxyproline content is a well-characterized assessment of the amount of fibrosis in tissues (Woessner, 1961). Bleomycin-treated rats that were dosed with 60 mg/kg of SD-208 showed a significant decrease in the total hydroxyproline per lung compared to the 1% methyl cellulose control (***$p < 0.001$). These results

Molecular Pharmacology Fast Forward. Published on May 17, 2006 as DOI: 10.1124/mol.105.021600
This article has not been copyedited and formatted. The final version may differ from this version.

demonstrate that TGFβ-receptor blockade, but not p38 inhibition, attenuates myofibroblast conversion and collagen deposition in an *in vivo* model of pulmonary fibrosis.

TGFβR1 Kinase Blockade Affects a Majority of TGFβ-responsive Genes in HLF Cells

We employed SD-208 and SD-282 together with cDNA microarray analysis to dissect the molecular signaling events downstream of the TGFβ pathway. Using these compounds, we tested the ability of each compound to affect TGFβ-regulated gene expression profiles in treated HLF cells at various times. A time course was performed in order comprehensively investigate the range of TGFβ response genes including the acute early gene changes as well as the later TGFβ events. Fluorescently labeled cDNAs were generated from four experimental groups at multiple time points to (1 h, 7.5 h, 24 h, and 72 h): unstimulated cells (control), TGFβ treated cells, TGFβ and SD-208 treated cells, TGFβ and SD-282 treated cells. The following hybridizations were performed in duplicate: control vs. TGFβ, TGFβ vs. TGFβ and SD-208, and TGFβ vs. TGFβ and SD-282. The 1 h samples were omitted from the inhibitor analysis, since TGFβ affected a small number of genes. As a result, this time point would not contribute significantly to a functional analysis of inhibitor-affected genes.

Molecular Pharmacology Fast Forward. Published on May 17, 2006 as DOI: 10.1124/mol.105.021600
This article has not been copyedited and formatted. The final version may differ from this version.

A time course of TGFβ-responsive genes was identified (Figure 8A). In terms of the number of genes affected by TGFβ, maximum changes were observed at 24 h (640 up- and 898 down-regulated). SD-208 had significant effects on gene expression induced by TGFβ; at 7.5 h, 24 h, and 72 h, the percentage of effected genes was 77%, 84%, and 58%, respectively (Figure 8B). In contrast, at these time points, SD-282 inhibited between 10-18% of TGFβ–regulated genes (Figure 8B). Most genes inhibited by SD-282 are also affected by SD-208 (Figure 8C), consistent with the expectation that the blockade of the TGFβR1 signaling affects the p38 MAPK pathway in TGFβ-simulated cells.

Taken together, these results show that SD-208, a potent inhibitor of TGFβR1, has striking affects on TGFβ–regulated gene expression. In contrast, p38 kinase inhibition opposed relatively few TGFβ-induced gene changes, suggesting that the p38 component of the TGFβ signaling pathway is relatively modest in human lung fibroblasts.

Gene Expression Clustering

Genes were grouped according to functional categories by using a combination of gene expression clustering and functional annotations (Figure 9).

Molecular Pharmacology Fast Forward. Published on May 17, 2006 as DOI: 10.1124/mol.105.021600
This article has not been copyedited and formatted. The final version may differ from this version.

Fibrosis and Extracellular Matrix Genes

A cluster of genes involved in fibrosis and extracellular matrix (ECM) deposition were regulated in response to TGFβ (Figure 9A). A majority of these genes were up-regulated by TGFβ. Representative examples include *CTGF, fibronectin, PAI-1, TIMP3, THBS2,* and several members of the Collagen gene family. All of these TGFβ-stimulated gene events were reversed by SD-208. SD-282 also showed a modest reversal of some of the genes in this cluster, such as *COMP (cartilage oligomeric matrix protein), TIMP3,* and *IL11*. These results show that SD-208 globally opposed TGFβ induced fibrotic gene expression in human lung fibroblasts, while SD-282 affected only a subset of the fibrogenic genes.

Inflammation Genes

Genes involved in inflammatory processes were elevated and repressed by TGFβ in HLF cells (Figure 9B). TGFβ stimulated pro-inflammatory genes including *COX2, COX1, IL6, interleukin 1 receptor accessory protein (IL1RAP), bradykinin receptor B2 (BDKRB2), tumor necrosis factor, alpha-induced protein 6 (TNFAIP6),* and *TNF superfamily, member 4 (TNFSF4).* At the same time, TGFβ also down-regulated pro-inflammatory genes such as *CCL13 (MCP-4), CXCL7 (MCP-3), CCL8 (MCP-2),* and *CXCL1 (GRO1)*. The effects of TGFβ on these genes increased over time: repression by TGFβ was not seen until 24 h (~4 - 6-fold) whereas, by 72 h the down-regulation increased to 8-11-fold. The TGFβ effects on all these gene regulatory events were

Molecular Pharmacology Fast Forward. Published on May 17, 2006 as DOI: 10.1124/mol.105.021600
This article has not been copyedited and formatted. The final version may differ from this version.

opposed by SD-208. Interestingly, ~30% of the TGFβ-regulated inflammatory genes were also reversed by SD-282. The genes, which are reversed by both inhibitors, include *COX2, IL1RAP, TNFAIP6, and TNFSF4*. Together, these data suggest that SD-208 and SD-282 attenuate TGFβ-induced pro-inflammatory gene responses in human lung fibroblasts.

Cytoskeletal Genes

A group of cytoskeletal genes was found to be regulated by TGFβ (Figure 9C). A majority of these genes are up-regulated by TGFβ. Representative genes from this cluster include known markers of myofibroblasts such as *α–smooth muscle actin 2 (ACTA2), α–skeletal muscle actin 1 (ACTA1),* and *non-muscle myosin heavy chain 9 (MYH9).* Many of the genes in this group are novel TGFβ-responsive genes. For example, TGFβ up-regulated *dystrophin* (*DMD*). DMD is involved in muscle contraction, which is an additional property that myofibroblasts acquire. SD-208, the TGFβR1 inhibitor, but not SD-282, the p38 MAPK inhibitor, opposed a majority of the TGFβ-induced cytoskeletal gene changes in this cluster. This result is consistent with the α–smooth muscle actin Western data showing that SD-208 blocks the transformation of fibroblasts to myofibroblasts. Furthermore, the temporal induction patterns of genes contributing to myofibroblast differentiation and contraction were up-regulated between 7.5 and 24 h consistent with our observation by Western analysis that α–smooth muscle

Molecular Pharmacology Fast Forward. Published on May 17, 2006 as DOI: 10.1124/mol.105.021600
This article has not been copyedited and formatted. The final version may differ from this version.

actin expression becomes detectable following treatment of fibroblasts with TGFβ by 24 h.

Cell Proliferation Genes

TGFβ regulated a cluster of genes involved in cell proliferation (Figure 9D). We found up-regulation of several genes including *CYR6 (IGFBP10), FGF2, IGF1, IGFBP7, PDGFA,* and *PTHLH*. The induction of these genes was suppressed by SD-208, but not by SD-282. In addition, down-regulation of several anti-proliferative genes such as *BTG1, CD164,* and *GAS1* was observed. The regulation of these genes was strongly suppressed by SD-208, and not by SD-282, except for *GAS1*, which showed modest reversal by SD-282. These data support a role for TGFβ in the positive regulation of cell proliferation in human lung fibroblasts following conversion to myofibroblasts in response to ligand mediated signaling through TGFβR1.

Apoptosis and Cell Survival Genes

TGFβ up-regulated anti-apoptotic genes including *BAG3, BNIP1, DAD1,* and *IER3* (Figure 9E). Additionally, TGFβ down-regulated numerous pro-apoptotic genes including *CASP5, CED-6, CRADD, DAP, DAPK2, HTATIP2, PLAGL1, REQ, STK17A, TIA1, TFPT,* and *TNFSF10.* All of these gene regulatory events were reversed by SD-208, while a subset, *DAP, REQ, TNFSF10,* and *STK17B,* was affected also by SD-282.

Molecular Pharmacology Fast Forward. Published on May 17, 2006 as DOI: 10.1124/mol.105.021600
This article has not been copyedited and formatted. The final version may differ from this version.

These results suggest that TGFβ may protect myofibroblasts from apoptosis in human lung fibroblasts, and that TGFβ receptor blockage relieves this protection.

TGFβ and MAPK Pathway Genes

TGFβ was also found to regulate genes within the TGFβ and MAPK pathways (Figure 9F and Supplemental Table E2). A majority of the genes were down-regulated by TGFβ, such as *MADH1 (mothers against DPP homolog 1 or SMAD1), TGFBR3 (betaglycan), MAP2K6 (MEK6), MAP3K5 (MEKK5), MAP4K4 (HGK),* and *MAPKAPK3 (3PK).* We also observed TGFβ repression of *SMAD3* (Table 3 and data not shown—one replicate at the 72 h TGFβ + SD-282 time point did not meet acceptable criteria as described in Methods). A few genes were up-regulated including *SKIL (SNO), MADH7 (SMAD7),* and *MAPK7 (ERK5*). All TGFβ induced gene expression changes in this group were reversed by SD-208. Interestingly, SD-282, the p38 MAPK inhibitor, also blocked TGFβ-down-regulation of *MEK6* and *MEKK5*, which activate p38 and JNK MAP kinases, respectively. Many of these gene changes represent novel TGFβ-induced events such as the regulation of *SNO, HGK*, and *3PK*. These results are consistent with ligand-induced feed back loops, which serve to regulate signaling, mediated by SMADs and p38 MAPK.

Molecular Pharmacology Fast Forward. Published on May 17, 2006 as DOI: 10.1124/mol.105.021600
This article has not been copyedited and formatted. The final version may differ from this version.

Validation of Microarray by Real-time RT-PCR and Western Analyses

Representative microarray data was validated in multiple HLF donors using real-time RT-PCR and Western analyses. The effects of TGFβ treatment and cotreatment with SD-208 or SD-282 were similar as measured by real-time RT-PCR and microarray for the tested genes: *ACTA2, TIMP3, CTGF, IL11, PAI-1, COX2, IL6, SMAD3, SMAD7, IER3, PDGFA, fibronectin,* and *IGF1* (Table 3, three separate donors). SD-208 reversed the TGFβ effects of these genes, whereas SD-282 showed effects only on a subset of genes including *TIMP3, IL11, COX2,* and *fibronectin*. Some differences between the microarray and real-time RT-PCR were noted for *fibronectin.* While TGFβ-induction of *fibronectin* was inhibited similarly by SD-208 using these two methods, partial inhibition by SD-282 was not detected by the differential expression threshold values of the microarray. Further validation of gene expression changes was observed at the protein level in two separate donors for CTGF, PAI-1, and α-smooth muscle actin (Figures 4 and 10, representative donor shown). Taken together, these results confirmed our microarray data using independent assay methods.

Molecular Pharmacology Fast Forward. Published on May 17, 2006 as DOI: 10.1124/mol.105.021600
This article has not been copyedited and formatted. The final version may differ from this version.

Discussion

Myofibroblasts play a key role in the pathogenesis of pulmonary fibrosis. Here, we demonstrate that a potent and selective inhibitor of TGFβR1, but not of p38 MAPK, blocked myofibroblast transformation in human lung fibroblasts and in an *in vivo* model of pulmonary fibrosis. The TGFβR1 inhibitor, SD-208, also reduced collagen deposition in a rat bleomycin model, suggesting SD-208 attenuates fibrosis in this model. Furthermore, blockade of TGFβR1, but not p38 MAPK, inhibited collagen gel contraction—a functional consequence of myofibroblast transformation. We also used cDNA microarray analysis to gain a better understanding of the molecular mechanisms downstream of TGFβR1 signaling as it relates in myofibroblast conversion in human lung fibroblasts.

Microarray analyses demonstrated that inhibition of TGFβR1 kinase activity by SD-208 opposed a majority (58–84%) of the TGFβ-induced gene expression changes from 7.5 h to 72 h. In contrast, blockade of the p38 MAPK pathway by SD-282 affected a minor subset (10-18%) of these TGFβ-mediated events during the same time course. TGFβR1 receptor blockade opposed TGFβ-regulated genes involved in fibrosis, myofibroblast transformation, cell proliferation, inflammation, and apoptosis. Inhibition of p38 MAPK demonstrated that a subset of the TGFβ-regulated events involved in inflammation and in fibrosis were mediated at least in part by p38.

Fibroblasts undergo transformation to myofibroblasts in response to TGFβ (Yokozeki et al., 1997). These smooth muscle-like cells are instrumental in

Molecular Pharmacology Fast Forward. Published on May 17, 2006 as DOI: 10.1124/mol.105.021600
This article has not been copyedited and formatted. The final version may differ from this version.

growth, development, and repair of normal and diseased tissues. During normal wound repair, myofibroblast transformation and expression of ECM proteins is initiated in response to injury, but terminates following healing when myofibroblasts disappear by apoptotic mechanisms (Desmouliere et al., 1995). In contrast in fibrotic diseases such as pulmonary fibrosis, myofibroblasts persist, as evident by fibroblastic foci in diseased lungs (Nicholson et al., 2002), with continued proliferation and ECM expression. This dysregulated state is sustained by the expression of profibrotic and proinflammatory factors including TGFβ, which act to prevent apoptosis and support continued expression of the factors by the myofibroblasts.

In the present study, we show that the process of myofibroblast transformation in human lung fibroblasts is dependent on signaling through the TGFβR1 and not the p38 pathway. The effects of inhibition of these pathways as they relate to myofibroblast conversion were measured by three independent methods: α-smooth muscle actin protein staining, microarray gene expression of cytoskeletal and muscle contraction genes, and collagen gel contraction. Collagen gel contraction assays are accepted as functionally relevant as models of fibrotic tissue remodeling because contraction induced by TGFβ during wound healing is thought to depend, in part, on the promotion of myofibroblast differentiation (Lijnen et al., 2003a; Lijnen et al., 2003b). We identified additional known markers (Manabe et al., 2002) of the conversion to myofibroblasts including *MYH9, tropomyosin 1,* and *tropomyosin 4* through microarray analysis (Table E2 and data not shown). Further supporting the transformation to the bonafide myofibroblast, we

Molecular Pharmacology Fast Forward. Published on May 17, 2006 as DOI: 10.1124/mol.105.021600
This article has not been copyedited and formatted. The final version may differ from this version.

found several newly identified TGFβ-responsive genes, which are involved in muscle contraction such as, *caldesmon 1, calponin 1, calponin 3, dystrophin,* and *troponin C* (Table E2 and data not shown). Induction of these genes by TGFβ was reversed by SD-208 and not SD-282. The observation that the p38 pathway is not involved in myofibroblast conversion is consistent with previous reports (Hashimoto et al., 2001; Horowitz et al., 2004). Taken together, these data corroborate the role of TGFβ in myofibroblast conversion and show that SD-208 attenuates this fibrogenic process.

Following activation of the myofibroblast by TGFβ, growth factors such as PDGF and CTGF, a member of the PDGF family, are thought to be responsible for myofibroblast proliferation (Powell et al., 1999). In the current study, we demonstrate that TGFβ induced the expression of *PDGFA* and *CTGF*, as well as several other growth factor genes, *IGFBP10, FGF2, IGF1, IGFBP7*, implicated in cell proliferation. Moreover, we found that TGFβ down-regulated several novel responsive genes (*BTG1, CD164, GAS1)* involved in anti-proliferative activities, further supporting its role in promoting myofibroblast proliferation. These TGFβ-regulated events were not affected by p38 inhibition, but were opposed by SD-208. Thus, TGFβ's role in myofibroblast proliferation is two-fold: induction of proliferative growth factors and suppression of genes that normally act to inhibit cell proliferation; both of these actions were effectively blocked by SD-208.

There is extensive literature implicating myofibroblasts as key sources of fibrotic gene expression and production of ECM. Although not fully investigated, there are

Molecular Pharmacology Fast Forward. Published on May 17, 2006 as DOI: 10.1124/mol.105.021600
This article has not been copyedited and formatted. The final version may differ from this version.

recent data suggesting that bone marrow derived progenitor cells in the lung may also be an important source of collagen production in pulmonary fibrosis (Hashimoto et al., 2004). Here, we show that in HLF cells, TGFβ induced the expression of ~20 genes involved in fibrogenic processes. Furthermore, we show that SD-208 globally opposes these fibrogenic gene changes. We found that a subset of the fibrotic genes (*TIMP3, IL11, fibronectin*) in myofibroblasts was regulated by both the TGFβ and p38 pathways. In most cases, the suppressive effects of SD-282 were modest compared to SD-208, suggesting that in a fibrogenic context, p38 pathway mediated events through TGFβR1 represent only partial signaling.

Myofibroblasts also play a major role in inflammatory responses (Phan et al., 1999). In the present study, we show that some of these effects are mediated by p38 signaling. We report for the first time that TGFβ up-regulation of several pro-inflammatory genes, *IL1RAP*, *TNFAIP6*, and *TNFSF4*, in HLF cells is mediated by the p38 pathway. We also observed that TGFβ induction of *COX2*, which is mediated in part by IL1RAP, is also opposed by SD-208 and SD-282. IL1RAP, interleukin 1 receptor accessory protein, forms a complex at the cell membrane with IL1 and its receptor, which is necessary for IL1 signal transduction. IL1 can mediate the induction of COX2 in intestinal fibroblasts (Mifflin et al., 2002) and the production of PGE2 in lung fibroblasts (Skold et al., 2000). Furthermore, we found that TGFβ down-regulated several pro-inflammatory genes, such as *MCP-4, MCP-3, MCP-2,* and *GRO1*, consistent with previous reports showing that TGFβ plays a dual role in inflammatory processes

Molecular Pharmacology Fast Forward. Published on May 17, 2006 as DOI: 10.1124/mol.105.021600
This article has not been copyedited and formatted. The final version may differ from this version.

(Bradbury et al., 2002; Fong et al., 2000; Gerritsma et al., 1998; Kitamura, 1997). Interestingly, the down-regulation of these genes increased over time. These results raise the possibility that TGFβ may have a role in the resolution of the inflammatory phase of the myofibroblast. Other genes relating to inflammatory processes that are down-regulated by TGFβ include several members of the steroid receptor family (*NR3C1/ glucocorticoid receptor*, *NR2C1, NR2F1, NR2F2)* (Table E2). The down-regulation of these genes is relieved by TGFβR1 receptor blockade, but not by p38 inhibition. Together, our results suggest that both TGFβ-induced SMAD signaling and p38 MAPK signaling are important in inflammatory responses in human lung fibroblasts. Moreover, the novel observation that effects of TGFβR1 blockade on steroid receptor genes raise the possibility that TGFβR1 inhibitors may be useful for increasing the efficacy of corticosteroids in inflammatory diseases such as asthma.

Successful wound repair mandates a process of myofibroblast elimination. This usually occurs after the proliferative and inflammatory phases subside. The mechanism of this resolution involves apoptosis (Desmouliere et al., 1995); however, the apoptotic process in the context of TGFβ signaling in myofibroblasts is not completely understood. Here we show that TGFβ regulated numerous apoptotic genes; TGFβ up-regulated anti-apoptotic genes and down-regulated pro-apoptotic genes. These gene groups also revealed several novel TGFβ-responsive genes such as *CED-6, CRADD, DAP, DAPK2, HTATIP2, PLAGL1, REQ,* and *STK17A.* In the context of extended TGFβ signaling, the gene changes suggest that TGFβ may serve to protect myofibroblasts from apoptosis.

Molecular Pharmacology Fast Forward. Published on May 17, 2006 as DOI: 10.1124/mol.105.021600
This article has not been copyedited and formatted. The final version may differ from this version.

These data are consistent with a previous report showing that TGFβ protects myofibroblasts against IL-1β-induced apoptosis (Zhang and Phan, 1999). SD-208 reversed the TGFβ-induced regulation of these apoptotic genes. The finding supports the notion that TGFβ-induced protection from apoptosis in human lung fibroblasts can be attenuated by TGFβR1 blockade and provides a rational for treating wounds susceptible to excessive scaring with inhibitors of TGFβR1.

In summary, our study demonstrates that SD-208, the TGFβR1 inhibitor, but not SD-282, the p38 MAPK inhibitor, attenuated TGFβ-induced: SMAD signaling and myofibroblast transformation *in vivo* and *in vitro*. Microarray analysis identified molecular fingerprints underlying these processes, and showed that SD-208 had global effects on reversing TGFβ-induced genes involved in fibrosis, inflammation, cell proliferation, cytoskeletal organization, and apoptosis. These studies also revealed that while the p38 pathway may not be needed for appearance or disappearance of the myofibroblast, it can mediate a subset of inflammatory and fibrogenic events of the myofibroblast during the process of tissue repair and fibrosis. Importantly, our studies support a therapeutic role for TGFβR1 inhibition in human interstitial lung diseases and support the use of inhibitors such as SD-208 for treating fibrotic conditions.

Molecular Pharmacology Fast Forward. Published on May 17, 2006 as DOI: 10.1124/mol.105.021600
This article has not been copyedited and formatted. The final version may differ from this version.

Acknowledgements.

The authors thank Lisa Garrard, Kip Madden, Jie Hu, and Estelle Tham for their informatics expertise and support, all of which made this work possible. In addition, we are grateful to Carl Dowds and Evelyn Lawani for their assistance in clone sequence verifications.

References.

Atfi A, Djelloul S, Chastre E, Davis R and Gespach C (1997) Evidence for a role of Rho-like GTPases and stress-activated protein kinase/c-Jun N-terminal kinase (SAPK/JNK) in transforming growth factor beta-mediated signaling. *J Biol Chem* 272(3):1429-1432.

Bakin AV, Rinehart C, Tomlinson AK and Arteaga CL (2002) p38 mitogen-activated protein kinase is required for TGFbeta-mediated fibroblastic transdifferentiation and cell migration. *J Cell Sci* 115(Pt 15):3193-3206.

Bakin AV, Tomlinson AK, Bhowmick NA, Moses HL and Arteaga CL (2000) Phosphatidylinositol 3-kinase function is required for transforming growth factor beta-mediated epithelial to mesenchymal transition and cell migration. *J Biol Chem* 275(47):36803-36810.

Bell E, Ivarsson B and Merrill C (1979) Production of a tissue-like structure by contraction of collagen lattices by human fibroblasts of different proliferative potential in vitro. *Proc Natl Acad Sci U S A* 76(3):1274-1278.

Bhowmick NA, Zent R, Ghiassi M, McDonnell M and Moses HL (2001) Integrin beta 1 signaling is necessary for transforming growth factor-beta activation of p38MAPK and epithelial plasticity. *J Biol Chem* 276(50):46707-46713.

Bonniaud P, Margetts PJ, Kolb M, Schroeder JA, Kapoun AM, Damm D, Murphy A, Chakravarty S, Dugar S, Higgins L, Protter AA and Gauldie J (2005) Progressive

Transforming Growth Factor {beta}1-induced Lung Fibrosis Is Blocked by an Orally Active ALK5 Kinase Inhibitor. *Am J Respir Crit Care Med* 171(8):889-898.

Bradbury DA, Newton R, Zhu YM, Stocks J, Corbett L, Holland ED, Pang LH and Knox AJ (2002) Effect of bradykinin, TGF-beta1, IL-1beta, and hypoxia on COX-2 expression in pulmonary artery smooth muscle cells. *Am J Physiol Lung Cell Mol Physiol* 283(4):L717-725.

Coker RK, Laurent GJ, Shahzeidi S, Lympany PA, du Bois RM, Jeffery PK and McAnulty RJ (1997) Transforming growth factors-beta 1, -beta 2, and -beta 3 stimulate fibroblast procollagen production in vitro but are differentially expressed during bleomycin-induced lung fibrosis. *Am J Pathol* 150(3):981-991.

Davies SP, Reddy H, Caivano M and Cohen P (2000) Specificity and mechanism of action of some commonly used protein kinase inhibitors. *Biochem J* 351(Pt 1):95-105.

Desmouliere A, Redard M, Darby I and Gabbiani G (1995) Apoptosis mediates the decrease in cellularity during the transition between granulation tissue and scar. *Am J Pathol* 146(1):56-66.

Fong CY, Pang L, Holland E and Knox AJ (2000) TGF-beta1 stimulates IL-8 release, COX-2 expression, and PGE(2) release in human airway smooth muscle cells. *Am J Physiol Lung Cell Mol Physiol* 279(1):L201-207.

Frey RS and Mulder KM (1997) Involvement of extracellular signal-regulated kinase 2 and stress-activated protein kinase/Jun N-terminal kinase activation by transforming growth factor beta in the negative growth control of breast cancer cells. *Cancer Res* 57(4):628-633.

Gerritsma JS, van Kooten C, Gerritsen AF, van Es LA and Daha MR (1998) Transforming growth factor-beta 1 regulates chemokine and complement production by human proximal tubular epithelial cells. *Kidney Int* 53(3):609-616.

Grande JP (1997) Role of transforming growth factor-beta in tissue injury and repair. *Proc Soc Exp Biol Med* 214(1):27-40.

Green FH (2002) Overview of pulmonary fibrosis. *Chest* 122(6 Suppl):334S-339S.

Hashimoto N, Jin H, Liu T, Chensue SW and Phan SH (2004) Bone marrow-derived progenitor cells in pulmonary fibrosis. *J Clin Invest* 113(2):243-252.

Hashimoto S, Gon Y, Takeshita I, Matsumoto K, Maruoka S and Horie T (2001) Transforming growth Factor-beta1 induces phenotypic modulation of human lung fibroblasts to myofibroblast through a c-Jun-NH2-terminal kinase-dependent pathway. *Am J Respir Crit Care Med* 163(1):152-157.

Hedges JC, Dechert MA, Yamboliev IA, Martin JL, Hickey E, Weber LA and Gerthoffer WT (1999) A role for p38(MAPK)/HSP27 pathway in smooth muscle cell migration. *J Biol Chem* 274(34):24211-24219.

Horowitz JC, Lee DY, Waghray M, Keshamouni VG, Thomas PE, Zhang H, Cui Z and Thannickal VJ (2004) Activation of the pro-survival phosphatidylinositol 3-

kinase/AKT pathway by transforming growth factor-beta1 in mesenchymal cells is mediated by p38 MAPK-dependent induction of an autocrine growth factor. *J Biol Chem* 279(2):1359-1367.

Iwasaki S, Iguchi M, Watanabe K, Hoshino R, Tsujimoto M and Kohno M (1999) Specific activation of the p38 mitogen-activated protein kinase signaling pathway and induction of neurite outgrowth in PC12 cells by bone morphogenetic protein-2. *J Biol Chem* 274(37):26503-26510.

Kapoun AM, Liang F, O'Young G, Damm DL, Quon D, White RT, Munson K, Lam A, Schreiner GF and Protter AA (2004) B-type natriuretic peptide exerts broad functional opposition to transforming growth factor-beta in primary human cardiac fibroblasts: fibrosis, myofibroblast conversion, proliferation, and inflammation. *Circ Res* 94(4):453-461.

Kitamura M (1997) Identification of an inhibitor targeting macrophage production of monocyte chemoattractant protein-1 as TGF-beta 1. *J Immunol* 159(3):1404-1411.

Kuroki S, Ohta A, Sueoka N, Katoh O, Yamada H and Yamaguchi M (1995) Determination of various cytokines and type III procollagen aminopeptide levels in bronchoalveolar lavage fluid of the patients with pulmonary fibrosis: inverse correlation between type III procollagen aminopeptide and interferon-gamma in progressive patients. *Br J Rheumatol* 34(1):31-36.

Li Z, Tran TT, Ma JY, O'Young G, Kapoun AM, Chakravarty S, Dugar S, Schreiner G and Protter AA (2004) p38 alpha mitogen-activated protein kinase inhibition

improves cardiac function and reduces myocardial damage in isoproterenol-induced acute myocardial injury in rats. *J Cardiovasc Pharmacol* 44(4):486-492.

Lijnen P, Petrov V and Fagard R (2003a) Transforming growth factor-beta 1-mediated collagen gel contraction by cardiac fibroblasts. *J Renin Angiotensin Aldosterone Syst* 4(2):113-118.

Lijnen P, Petrov V, Rumilla K and Fagard R (2003b) Transforming growth factor-beta 1 promotes contraction of collagen gel by cardiac fibroblasts through their differentiation into myofibroblasts. *Methods Find Exp Clin Pharmacol* 25(2):79-86.

Ludwicka A, Ohba T, Trojanowska M, Yamakage A, Strange C, Smith EA, Leroy EC, Sutherland S and Silver RM (1995) Elevated levels of platelet derived growth factor and transforming growth factor-beta 1 in bronchoalveolar lavage fluid from patients with scleroderma. *J Rheumatol* 22(10):1876-1883.

Manabe I, Shindo T and Nagai R (2002) Gene expression in fibroblasts and fibrosis: involvement in cardiac hypertrophy. *Circ Res* 91(12):1103-1113.

Massague J, Attisano L and Wrana JL (1994) The TGF-beta family and its composite receptors. *Trends Cell Biol* 4(5):172-178.

Mifflin RC, Saada JI, Di Mari JF, Adegboyega PA, Valentich JD and Powell DW (2002) Regulation of COX-2 expression in human intestinal myofibroblasts: mechanisms of IL-1-mediated induction. *Am J Physiol Cell Physiol* 282(4):C824-834.

Mio T, Adachi Y, Romberger DJ, Ertl RF and Rennard SI (1996) Regulation of fibroblast proliferation in three-dimensional collagen gel matrix. *In Vitro Cell Dev Biol Anim* 32(7):427-433.

Mio T, Liu XD, Adachi Y, Striz I, Skold CM, Romberger DJ, Spurzem JR, Illig MG, Ertl R and Rennard SI (1998) Human bronchial epithelial cells modulate collagen gel contraction by fibroblasts. *Am J Physiol* 274(1 Pt 1):L119-126.

Monzen K, Shiojima I, Hiroi Y, Kudoh S, Oka T, Takimoto E, Hayashi D, Hosoda T, Habara-Ohkubo A, Nakaoka T, Fujita T, Yazaki Y and Komuro I (1999) Bone morphogenetic proteins induce cardiomyocyte differentiation through the mitogen-activated protein kinase kinase kinase TAK1 and cardiac transcription factors Csx/Nkx-2.5 and GATA-4. *Mol Cell Biol* 19(10):7096-7105.

Nakamura K, Shirai T, Morishita S, Uchida S, Saeki-Miura K and Makishima F (1999) p38 mitogen-activated protein kinase functionally contributes to chondrogenesis induced by growth/differentiation factor-5 in ATDC5 cells. *Exp Cell Res* 250(2):351-363.

Nicholson AG, Fulford LG, Colby TV, du Bois RM, Hansell DM and Wells AU (2002) The relationship between individual histologic features and disease progression in idiopathic pulmonary fibrosis. *Am J Respir Crit Care Med* 166(2):173-177.

Phan SH (2002) The myofibroblast in pulmonary fibrosis. *Chest* 122(6 Suppl):286S-289S.

Phan SH, Zhang K, Zhang HY and Gharaee-Kermani M (1999) The myofibroblast as an inflammatory cell in pulmonary fibrosis. *Curr Top Pathol* 93:173-182.

Powell DW, Mifflin RC, Valentich JD, Crowe SE, Saada JI and West AB (1999) Myofibroblasts. I. Paracrine cells important in health and disease. *Am J Physiol* 277(1 Pt 1):C1-9.

Skold CM, Liu XD, Umino T, Zhu YK, Ertl RF, Romberger DJ and Rennard SI (2000) Blood monocytes attenuate lung fibroblast contraction of three-dimensional collagen gels in coculture. *Am J Physiol Lung Cell Mol Physiol* 279(4):L667-674.

Sporn MB and Roberts AB (1992) Transforming growth factor-beta: recent progress and new challenges. *J Cell Biol* 119(5):1017-1021.

Thrall RS, McCormick JR, Jack RM, McReynolds RA and Ward PA (1979) Bleomycin-induced pulmonary fibrosis in the rat: inhibition by indomethacin. *Am J Pathol* 95(1):117-130.

Woessner JF, Jr. (1961) The determination of hydroxyproline in tissue and protein samples containing small proportions of this imino acid. *Arch Biochem Biophys* 93:440-447.

Yang IV, Chen E, Hasseman JP, Liang W, Frank BC, Wang S, Sharov V, Saeed AI, White J, Li J, Lee NH, Yeatman TJ and Quackenbush J (2002) Within the fold: assessing differential expression measures and reproducibility in microarray assays. *Genome Biol* 3(11):research0062.

Yokozeki M, Moriyama K, Shimokawa H and Kuroda T (1997) Transforming growth factor-beta 1 modulates myofibroblastic phenotype of rat palatal fibroblasts in vitro. *Exp Cell Res* 231(2):328-336.

Zhang HY and Phan SH (1999) Inhibition of myofibroblast apoptosis by transforming growth factor beta(1). *Am J Respir Cell Mol Biol* 21(6):658-665.

Molecular Pharmacology Fast Forward. Published on May 17, 2006 as DOI: 10.1124/mol.105.021600
This article has not been copyedited and formatted. The final version may differ from this version.

Figure Legends

Figure 1. Structures of SD-208 and SD-282.

Figure 2. Effects of SD-208 and SD-282 on TGFβ-induced SMAD2/3 phosphorylation in HLF cells. Cells were treated with TGFβ for 30 minutes in the presence of multiple concentrations (0-400 nmol/L) of SD-208 (A, C) or SD-282 (B, D). SMAD phosphorylation was measured by ELISA (A, B) and Western blot analysis (C, D) using antibodies for SMAD2/3 and SMAD2, respectively. Analysis are presented as mean±SD from 3 or 4 separate experiments. Relative responses for each curve (C and D) were determined by defining the p-Smad response for TGFβ-treated + 0 nM compound as 100%. Band densities (C and D) were quantitated by Image Quant 5.2. Statistical significance (*** $P<0.001$, ** $P<0.01$, and * $P<0.05$) was determined for each treatment relative to TGFβ-treated + 0 nM (below the line) and relative to the next lower inhibitor concentration (above the line).

Figure 3. Effects of SD-208 and SD-282 on TGFβ-induced SMAD2 nuclear translocation in human lung fibroblasts. Human lung fibroblast cells were treated in the presence or absence of TGFβ for 30 minutes with or without SD-208 (200 nmol/L) or SD-282 (200 nmol/L).

Molecular Pharmacology Fast Forward. Published on May 17, 2006 as DOI: 10.1124/mol.105.021600
This article has not been copyedited and formatted. The final version may differ from this version.

Figure 4. Inhibition of α–smooth muscle actin protein expression. Protein levels of α–smooth muscle actin were measured by Western blot analysis from HLF cells treated for 24 h (A, B) and 72 h (C, D) with TGFβ in the presence of either SD-208 (400 nmol/L) or SD-282 (400 nmol/L). The histograms in (A) and (C) represent mean data points from two separate experiments each including triplicate biological replicates (n=5-6, mean±SD). The data is normalized to GAPDH and expressed as a percent compared to the TGFβ-treated samples. (B) and (D) are representative Western blots showing α–smooth muscle actin (α-SMA) and GAPDH protein staining. *** $P<0.001$, ** $P<0.01$, * $P<0.05$ vs. TGFβ.

Figure 5. Effects of SD-208 and SD-282 on TGFβ-induced collagen gel contraction. HLF cells were cast in 3-dimensional collagen gels. Gels were released into media with and without TGFβ in the presence or absence of SD-208 (A) or SD-282 (B). After 2 days of culture, the area of the floating gels was measured with an image analyzer. Data are presented as a means +/-SE of three replicate gels for each condition; ***$P=<0.001$ vs. TGFβ–treated control (SF-FBS). Statistical significance ($P=<0.001$) between inhibitor doses was observed for the following comparisons: the TGFβ+ SD-208 group (25 vs. 100 nmol/L, 25 vs. 200 nmol/L, 50 vs. 100 nmol/L, 50 vs. 200 nmol/L); the SD-208 group (25 vs. 200 nmol/L), and the TGFβ+ SD-282 group (50 vs. 100 nmol/L).

Molecular Pharmacology Fast Forward. Published on May 17, 2006 as DOI: 10.1124/mol.105.021600
This article has not been copyedited and formatted. The final version may differ from this version.

Figure 6. Histology of lungs from bleomycin-treated rats +/- SD-208 and SD-282. The animals were sacrificed 14 days after instillation of bleomycin or vehicle. The lungs were stained by immunohistochemistry with α–smooth muscle actin. (A) Saline + 1% MC; (B) Bleo + 1% MC; (C) Bleo + SD-208 (60 mg/kg); (D) Saline + 1% PEG-400; (E) Bleo + 1% PEG-400; (F) Bleo + SD-282 (60 mg/kg). Magnifications shown for A-F are ×400. Histograms (bottom) represent the number of myofibroblasts at the fibroblastic foci (mean +/- SD for 36-40 fields from each of 3-4 animals). Statistical significance ($P<0.01$, unpaired student's t-test) was achieved for the SD-208 versus vehicle group.

Figure 7. Collagen deposition as a measure of fibrosis in bleomycin-treated rats. The animals were sacrificed 14 days after instillation of bleomycin or vehicle. Hydroxyproline content in whole lungs was measured in all animals (7 to 8 animals per group). Bleomycin-treated rats dosed with 60 mg/kg of SD-208 showed a significant decrease in the total hydroxyproline per lung compared to the 1% methyl cellulose control (***$P < 0.001$).

Figure 8. Microarray analysis in TGFβ-treated HLF cells. (A) Gene expression changes induced by TGFβ and in HLF cells at 1, 7.5, 24 and 72 h. Histograms show the number of gene expression changes that were up-regulated and down-regulated by TGFβ treatment. Hybridizations using fluorescently-labeled cDNA probes compare untreated (control) to TGFβ-treated cells. Histogram bars: up-regulated genes (black) and down-

regulated genes (grey). (B) Effects of SD-208 (400 nmol/L) and SD-282 (400 nmol/L) on TGFβ-induced gene expression. Hybridizations using fluorescently-labeled cDNA probes compare TGFβ-treated to TGFβ+ inhibitor-treated cells at 7.5, 24, and 72 h. See Methods for details related to statistical significance. Histogram bars: no inhibitor effect and inhibitor effect (black). (C) Venn diagram showing overlap of TGFβ-induced gene expression changes affected by SD-208 and/or SD-282 at 7.5, 24, and 72 h.

Figure 9. Gene expression clusters in HLF cells: (A) Fibrosis and ECM, (B) Inflammation (C) Cytoskeletal (D) Cell proliferation (E) Apoptosis and Cell survival (F) TGFβ and p38 MAPK pathway. Each column represents the results from duplicate hybridizations: (1) control vs. TGFβ, 1 h; (2) control vs. TGFβ, 7.5 h; (3) control vs. TGFβ, 24 h; (4) control vs. TGFβ, 72 h; (5) TGFβ vs. TGFβ + SD-208, 7.5 h; (6) TGFβ vs. TGFβ + SD-208, 24 h; (7) TGFβ vs. TGFβ + SD-208, 72 h; (8) TGFβ vs. TGFβ + SD-282, 7.5 h; (9) TGFβ vs. TGFβ + SD-282, 24 h; (10) TGFβ vs. TGFβ + SD-282, 72 h. Normalized data values depicted in shades of red and green represent elevated and repressed expression, respectively. Data was generated using the hierarchical clustering algorithm contained in Spotfire™ software. See Supplemental Table E2 for gene identities and expression values.

Figure 10. Effects of SD-208 and SD-282 on TGFβ-induced PAI-1 and CTGF. Protein levels of PAI-1 (A, B) and CTGF (C-F) were measured by ELISA and Western blot

analysis, respectively. Human lung fibroblast cells were treated with TGFβ in the presence of either SD-208 (400 nmol/L) or SD-282 (400 nmol/L) for 24h (A, C, D) and 72 h (B, E, F). The histograms in A, B, C, and E represent mean data points from two separate experiments each including triplicate biological replicates (n=6). The Western blot data is normalized to Vimentin and expressed as a percent compared to the TGFβ-treated samples. D and F are representative Western blots showing CTGF and Vimentin protein staining. $^{***}P$=<0.001, $^{**}P$<0.01 vs. TGFβ.

Molecular Pharmacology Fast Forward. Published on May 17, 2006 as DOI: 10.1124/mol.105.021600
This article has not been copyedited and formatted. The final version may differ from this version.

Table 1. Specificity of SD-208 for TGFβR1 kinase activity

Kinase Target	IC_{50} or % Inhbition*
TGFβR1	0.0485
TGFβR2	22%
p38α	0.854
p38β	1.92
EGFR Kinase	0.686
p38γ	0%
JNK1	0%
MAPKAPK2	29%
MKK6	37%
ERK2	20%
PKA	15%
PKC	0%
PKD	6%
CDC2	61%
CaMKII	10%

*Data are expressed as IC_{50} (μmol/L) or percentage inhibition at 50 μmol/L SD-208 based on direct enzymatic assay

Molecular Pharmacology Fast Forward. Published on May 17, 2006 as DOI: 10.1124/mol.105.021600
This article has not been copyedited and formatted. The final version may differ from this version.

Table 2. Specificity of SD-282 for p38 MAPK activity

Kinase Target	IC50 or % Inhbition*
p38α	0.00161
p38β	0.023
p38γ	14% at 10uM
p38δ	0% at 10uM
MAPKAPK2	31% at 50uM
MKK6	28% at 50uM
ERK2	0% at 50uM
PKA	0% at 50uM
PKC	0% at 50uM
PKD	0% at 50uM
CDC2	0% at 50uM
CaMKII	48% at 50uM
JNK1	0% at 50uM
TGFβR1	0% at 50uM
EGFR kinase	0% at 50uM

*Data are expressed as IC_{50} (μmol/L) or percentage inhibition based on direct enzymatic assay

Molecular Pharmacology Fast Forward. Published on May 17, 2006 as DOI: 10.1124/mol.105.021600
This article has not been copyedited and formatted. The final version may differ from this version.

Table 3 Gene expression assayed by real-time RT-PCR.

Gene	Donor	Control	SD-208	SD-282	TGFβ	SD-208 + TGFβ	SD-282 + TGFβ	Time (h)
PAI-1	*A*	1.0 ± 0.1	0.5 ± 0.1	1.0 ± 0.1	16.1 ± 0.8	1.3 ± 0.1	17.0 ± 0.7	24
		1.0 ± 0.1	0.7 ± 0.1	1.6 ± 0.4	9.2 ± 1.2	3.6 ± 0.5	9.9 ± 1.1	72
	B	1.0 ± 0.0	0.3 ± 0.0	0.9 ± 0.1	9.2 ± 0.5	1.1 ± 0.1	11.1 ± 0.7	24
		1.0 ± 0.1	0.3 ± 0.0	1.0 ± 0.1	5.3 + 0.2	2.0 + 0.2	5.9 + 0.2	72
	C	1.0 ± 0.1	0.4 ± 0.0	1.0 ± 0.1	12.7 ± 0.7	1.4 ± 0.0	14.8 ± 1.3	24
		1.0 ± 0.1	0.6 ± 0.0	1.1 ± 0.2	6.0 ± 0.5	3.4 ± 0.0	7.8 ± 1.0	72
Fibronectin	*A*	1.0 ± 0.2	0.9 ± 0.0	0.7 ± 0.2	2.4 ± 0.2	1.0 ± 0.1	1.5 ± 0.1	24
		1.0 ± 0.1	0.9 ± 0.3	1.4 ± 0.6	5.2 ± 0.4	1.5 ± 0.3	3.1 ± 0.7	72
	B	1.0 ± 0.2	0.7 ± 0.1	1.0 ± 0.0	2.2 ± 0.4	0.8 ± 0.1	1.6 ± 0.1	24
		1.0 ± 0.2	0.6 ± 0.1	0.9 ± 0.2	2.9 ± 0.2	1.2 ± 0.2	2.3 ± 0.2	72
	C	1.0 ± 0.2	0.8 ± 0.1	0.8 ± 0.1	2.1 ± 0.1	1.1 ± 0.1	1.5 ± 0.3	24
		1.0 ± 0.1	0.8 ± 0.0	0.8 ± 0.2	2.7 ± 0.2	1.4 ± 0.0	1.9 ± 0.2	72
CTGF	*A*	1.0 ± 0.1	0.5 ± 0.1	1.3 ± 0.1	17.2 ± 0.5	2.0 ± 0.3	18.5 ± 3.8	24
		1.0 ± 0.3	1.0 ± 0.3	1.9 ± 0.6	6.9 ± 0.3	4.0 ± 0.5	9.4 ± 1.6	72
	B	1.0 ± 0.1	0.3 ± 0.1	1.1 ± 0.1	7.0 ± 1.5	1.0 ± 0.1	7.1 ± 1.4	24
		1.0 ± 0.1	0.5 ± 0.0	1.2 ± 0.0	3.5 ± 0.1	1.8 ± 0.2	4.5 ± 0.1	72
	C	1.0 ± 0.1	0.3 ± 0.0	1.1 ± 0.1	14.0 ± 0.5	1.7 ± 0.1	15.4 ± 0.9	24
		1.0 ± 0.0	0.7 ± 0.1	1.2 ± 0.1	5.3 ± 0.4	3.5 ± 0.2	6.5 ± 1.0	72
IL6	*A*	1.0 ± 0.3	0.7 ± 0.1	1.0 ± 0.1	3.5 ± 0.2	1.0 ± 0.2	4.0 ± 0.2	24
		1.0 ± 0.3	1.1 ± 0.3	1.7 ± 0.6	0.8 ± 0.1	1.5 ± 0.1	1.6 ± 0.1	72
	B	1.0 ± 0.0	0.6 ± 0.2	0.7 ± 0.2	3.7 ± 0.5	0.9 ± 0.2	4.7 ± 0.8	24
		1.0 ± 0.2	0.6 ± 0.1	0.8 ± 0.1	2.0 ± 0.1	1.3 ± 0.2	2.4 ± 0.3	72
	C	1.0 ± 0.0	0.6 ± 0.1	0.9 ± 0.0	3.6 ± 0.4	1.1 ± 0.1	4.9 ± 0.4	24
		1.0 ± 0.0	0.9 ± 0.1	0.9 ± 0.1	0.9 ± 0.1	1.3 ± 0.0	1.3 ± 0.2	72
IL11	*A*	1.0 ± 0.2	0.8 ± 0.1	0.8 ± 0.1	147.7 ± 15.3	1.5 ± 0.4	121.9 ± 7.8	24
		1.0 ± 0.2	0.8 ± 0.2	0.8 ± 0.0	33.0 ± 4.4	3.0 ± 0.1	24.4 ± 5.2	72
	B	1.0 ± 0.1	0.7 ± 0.2	0.7 ± 0.1	52.0 ± 8.5	1.1 ± 0.2	38.8 ± 6.6	24
		1.0 ± 0.1	0.9 ± 0.3	0.9 ± 0.2	13.5 ± 1.6	1.9 ± 0.2	8.6 ± 1.2	72
	C	1.0 ± 0.1	1.0 ± 0.1	1.0 ± 0.0	51.3 ± 2.1	1.4 ± 0.1	38.5 ± 3.2	24
		1.0 ± 0.1	1.0 ± 0.2	1.0 ± 0.2	10.4 ± 1.0	2.1 ± 0.1	7.4 ± 0.6	72

Molecular Pharmacology Fast Forward. Published on May 17, 2006 as DOI: 10.1124/mol.105.021600
This article has not been copyedited and formatted. The final version may differ from this version.

	A	1.0 ± 0.2	1.1 ± 0.1	0.9 ± 0.1	0.2 ± 0.0	0.9 ± 0.1	0.1 ± 0.0	24
SMAD3		1.0 ± 0.2	1.1 ± 0.1	1.1 ± 0.1	0.2 ± 0.0	0.8 ± 0.1	0.2 ± 0.0	72
	B	1.0 ± 0.2	0.9 ± 0.3	0.8 ± 0.2	0.2 ± 0.0	0.9 ± 0.1	0.2 ± 0.0	24
		1.0 ± 0.1	1.0 ± 0.1	1.2 ± 0.2	0.2 ± 0.0	1.0 ± 0.1	0.2 ± 0.0	72
	C	1.0 ± 0.1	1.1 ± 0.1	0.9 ± 0.0	0.2 ± 0.0	1.1 ± 0.2	0.2 ± 0.1	24
		1.0 ± 0.1	1.0 ± 0.1	0.9 ± 0.2	0.2 ± 0.0	0.6 ± 0.1	0.2 ± 0.0	72
	A	1.0 ± 0.2	0.9 ± 0.2	1.0 ± 0.1	5.9 ± 0.4	1.5 ± 0.2	5.3 ± 0.4	24
SMAD7		1.0 ± 0.2	0.9 ± 0.2	1.1 ± 0.3	5.1 ± 0.9	1.7 ± 0.1	4.4 ± 0.2	72
	B	1.0 ± 0.2	0.7 ± 0.2	0.8 ± 0.2	2.7 ± 0.1	1.2 ± 0.3	3.1 ± 0.5	24
		1.0 ± 0.3	0.9 ± 0.1	1.2 ± 0.2	3.0 ± 0.3	1.6 ± 0.2	3.4 ± 0.2	72
	C	1.0 ± 0.0	0.9 ± 0.1	1.0 ± 0.0	5.0 ± 0.5	1.5 ± 0.0	4.5 ± 0.3	24
		1.0 ± 0.1	0.8 ± 0.2	0.9 ± 0.1	3.7 ± 0.4	1.6 ± 0.1	3.4 ± 0.3	72
	A	1.0 ± 0.1	0.9 ± 0.2	0.8 ± 0.1	11.1 ± 0.7	0.9 ± 0.1	6.7 ± 0.1	24
COX2		1.0 ± 0.2	0.9 ± 0.2	0.9 ± 0.2	3.9 ± 1.4	1.3 ± 0.3	3.1 ± 0.3	72
	B	1.0 ± 0.1	1.1 ± 0.2	0.9 ± 0.2	6.2 ± 0.5	1.2 ± 0.2	2.8 ± 0.1	24
		1.0 ± 0.2	1.2 ± 0.1	0.9 ± 0.1	4.4 ± 0.1	1.1 ± 0.0	2.3 ± 0.4	72
	C	1.0 ± 0.0	1.4 ± 0.2	1.0 ± 0.1	6.8 ± 0.4	1.8 ± 0.1	3.6 ± 0.1	24
		1.0 ± 0.2	1.4 ± 0.3	0.9 ± 0.2	2.1 ± 0.1	1.3 ± 0.1	1.3 ± 0.3	72
	A	1.0 ± 0.2	0.9 ± 0.3	1.0 ± 0.1	9.5 ± 1.8	0.8 ± 0.1	3.3 ± 0.4	24
TIMP3		1.0 ± 0.2	1.0 ± 0.1	0.9 ± 0.1	12.4 ± 1.3	1.1 ± 0.2	3.9 ± 0.3	72
	B	1.0 ± 0.1	0.8 ± 0.2	0.9 ± 0.2	13.0 ± 1.5	0.9 ± 0.1	8.4 ± 1.4	24
		1.0 ± 0.2	0.9 ± 0.0	0.9 ± 0.1	17.8 ± 0.6	1.2 ± 0.0	5.1 ± 0.8	72
	C	1.0 ± 0.1	0.9 ± 0.1	0.7 ± 0.0	11.5 ± 0.4	1.3 ± 0.1	7.5 ± 1.1	24
		1.0 ± 0.1	0.9 ± 0.2	0.8 ± 0.2	10.7 ± 0.8	1.9 ± 0.1	5.9 ± 0.7	72
	A	1.0 ± 0.1	0.6 ± 0.1	1.0 ± 0.1	9.8 ± 1.1	0.9 ± 0.1	7.9 ± 1.1	24
ACTA2		1.0 ± 0.1	0.7 ± 0.1	1.0 ± 0.2	3.7 ± 1.4	2.3 ± 0.6	5.9 ± 1.4	72
	B	1.0 ± 0.1	0.3 ± 0.0	1.0 ± 0.3	8.4 ± 1.7	0.7 ± 0.1	7.3 ± 0.5	24
		1.0 ± 0.2	0.5 ± 0.0	1.4 ± 0.0	9.8 ± 0.6	1.8 ± 0.4	9.7 ± 1.7	72
	C	1.0 ± 0.3	0.7 ± 0.2	1.2 ± 0.3	12.3 ± 0.6	1.1 ± 0.1	11.8 ± 0.8	24
		1.0 ± 0.1	0.8 ± 0.1	1.2 ± 0.3	9.9 ± 0.8	4.0 ± 0.9	9.8 ± 1.1	72
	A	1.0 ± 0.3	0.7 ± 0.1	1.0 ± 0.5	6.9 ± 0.7	1.8 ± 0.5	7.2 ± 2.2	24
IER3		1.0 ± 0.2	0.7 ± 0.1	1.3 ± 0.6	4.8 ± 2.4	2.2 ± 1.1	5.8 ± 1.8	72

Molecular Pharmacology Fast Forward. Published on May 17, 2006 as DOI: 10.1124/mol.105.021600
This article has not been copyedited and formatted. The final version may differ from this version.

	B	1.0 ± 0.1	0.7 ± 0.2	0.8 ± 0.2	3.2 ± 0.4	1.2 ± 0.2	4.3 ± 0.9	24
		1.0 ± 0.2	0.8 ± 0.0	1.2 ± 0.1	2.6 ± 0.2	1.9 ± 0.1	3.7 ± 0.2	72
	C	1.0 ± 0.5	0.6 ± 0.1	0.8 ± 0.1	3.7 ± 0.5	1.3 ± 0.1	4.6 ± 1.0	24
		1.0 ± 0.1	1.0 ± 0.1	1.2 ± 0.0	3.0 ± 0.2	2.7 ± 0.1	4.5 ± 0.3	72
	A	1.0 ± 0.2	0.7 ± 0.1	1.0 ± 0.4	3.8 ± 0.4	1.2 ± 0.1	3.2 ± 0.3	24
PDGFA		1.0 ± 0.3	0.7 ± 0.1	0.9 ± 0.2	1.5 ± 0.4	1.5 ± 0.7	1.8 ± 0.5	72
	B	1.0 ± 0.1	0.6 ± 0.1	0.7 ± 0.1	3.9 ± 0.2	0.8 ± 0.1	3.5 ± 0.6	24
		1.0 ± 0.1	0.7 ± 0.0	1.0 ± 0.1	2.2 ± 0.1	1.1 ± 0.1	2.2 ± 0.1	72
	C	1.0 ± 0.1	0.9 ± 0.0	0.9 ± 0.1	5.0 ± 0.2	1.1± 0.2	4.8 ± 0.3	24
		1.0 ± 0.1	0.9 ± 0.1	0.9 ± 0.1	1.9 ± 0.1	1.5 ± 0.3	1.8 ± 0.2	72
	A	1.0 ± 0.4	0.1 ± 0.1	0.9 ± 0.4	22.7 ± 4.8	5.7 ± 1.6	31.0 ± 7.4	24
IGF1		1.0 ± 0.3	0.0 ± 0.0	0.8 ± 0.5	12.1 ± 6.8	6.9 ± 3.1	18.3 ± 7.1	72
	B	1.0 ± 0.1	0.0 ± 0.0	0.9 ± 0.4	14.1 ± 1.7	2.1 ± 0.4	15.7 ± 2.2	24
		1.0 ± 0.2	0.5 ± 0.8	1.0 ± 0.9	22.3 ± 0.9	6.6 ± 1.2	26.4 ± 3.4	72
	C	1.0 ± 0.1	0.3 ± 0.0	0.8 ± 0.1	15.7 ± 0.0	3.3 ± 0.6	20.5 ± 3.2	24
		1.0 ± 0.1	0.3 ± 0.0	1.0 ± 0.0	16.4 ± 0.6	7.7 ± 0.6	23.0 ± 4.9	72

Figure 1

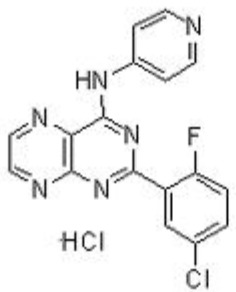

SD-208

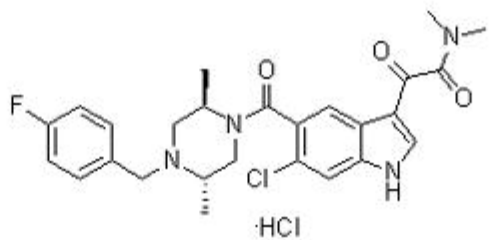

SD-282

Figure 2

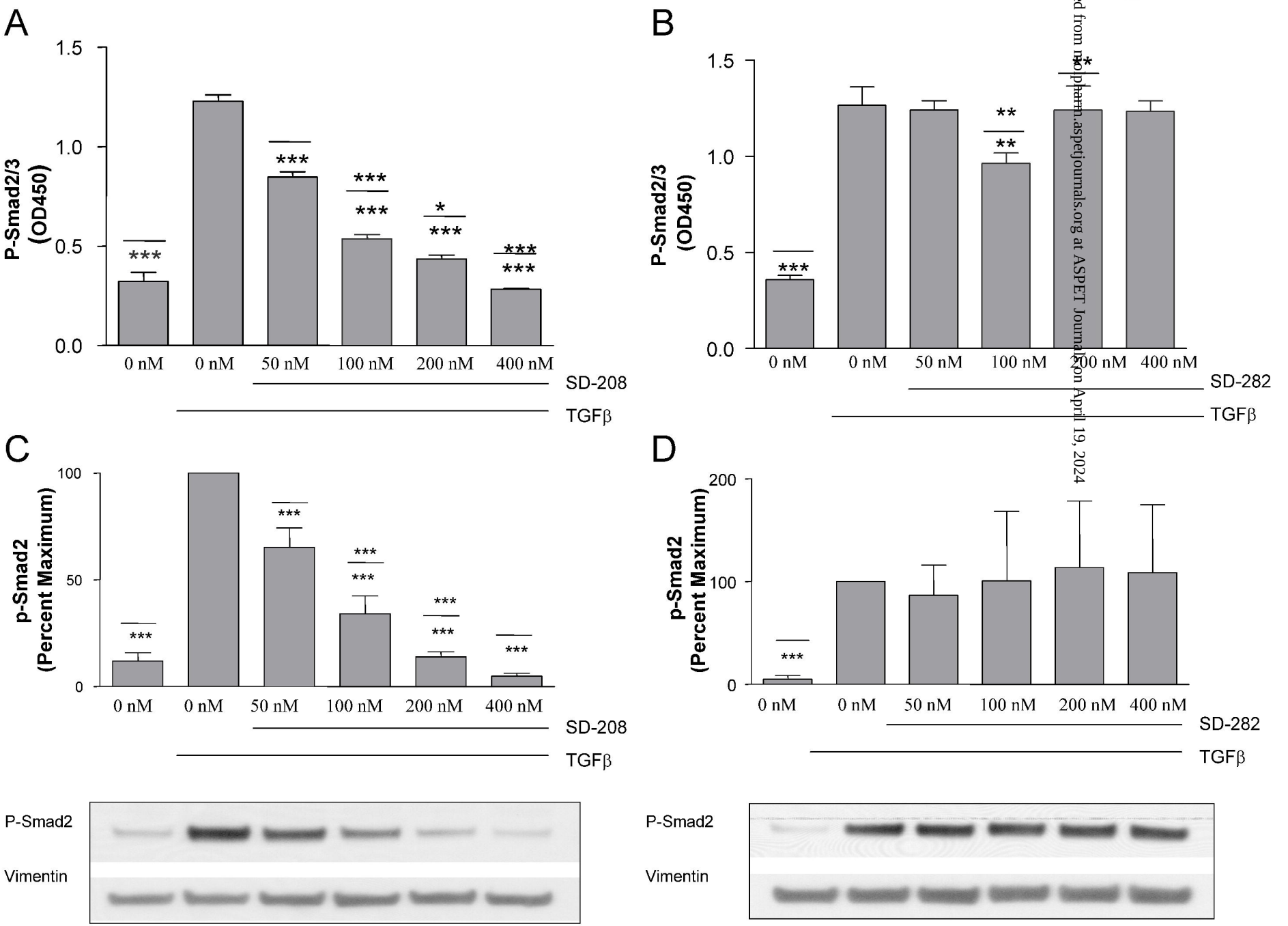

Figure 3

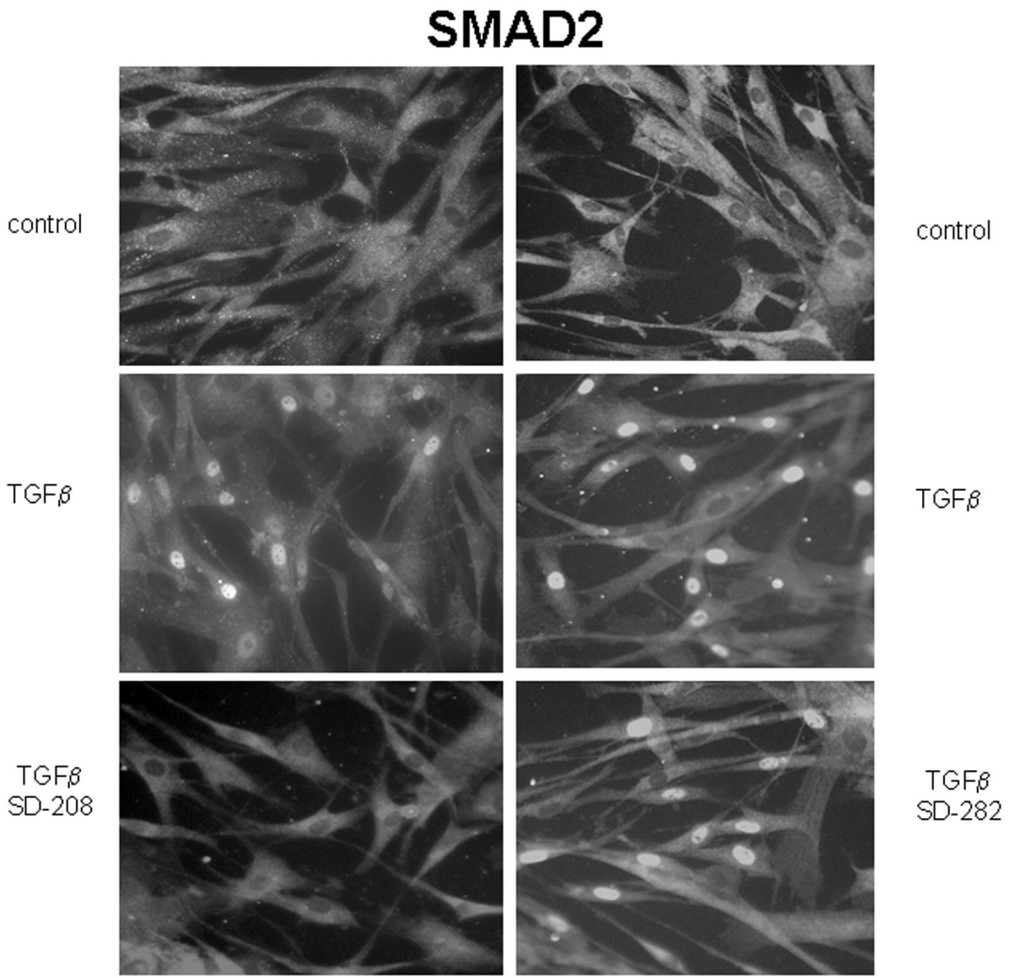

Figure 4

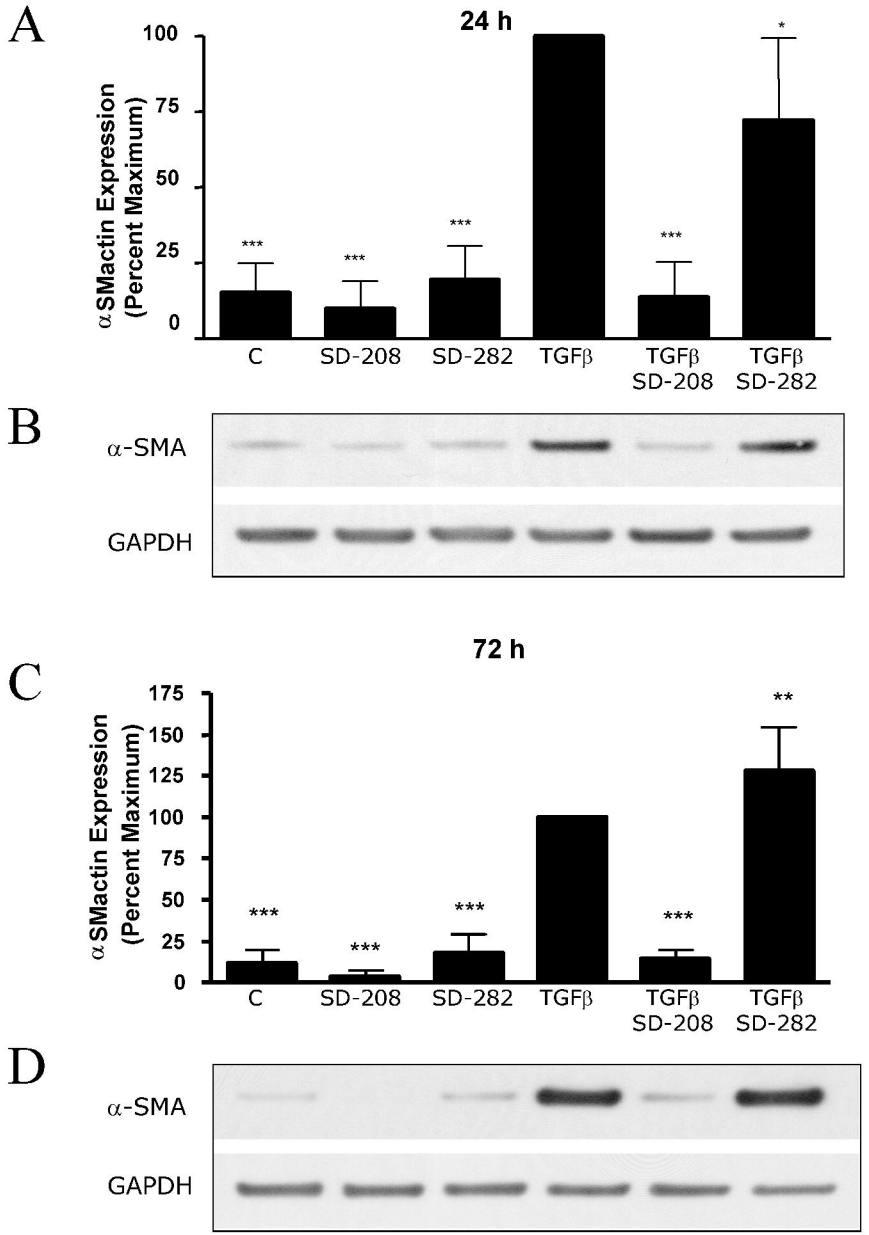

Figure 5

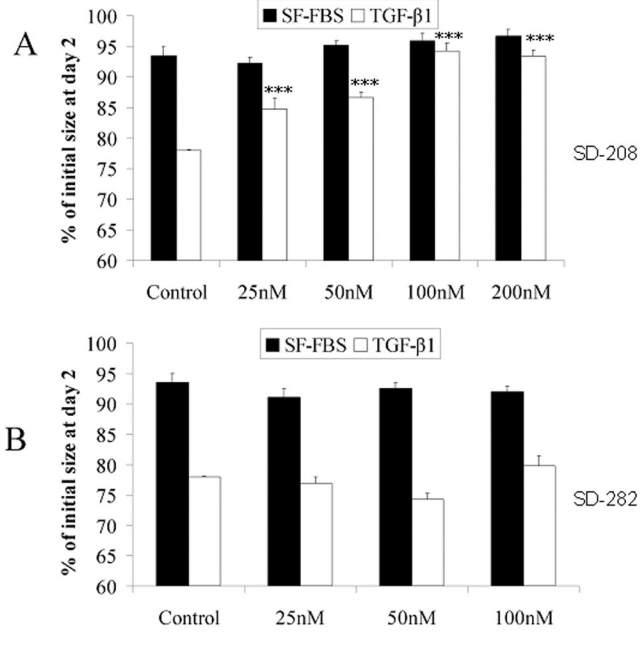
A
SF-FBS
TGF-β1
% of initial size at day 2
100
95
90
85
80
75
70
65
60
***
***
***
***
SD-208
Control
25nM
50nM
100nM
200nM
B
SF-FBS
TGF-β1
% of initial size at day 2
100
95
90
85
80
75
70
65
60
SD-282
Control
25nM
50nM
100nM

Figure 6

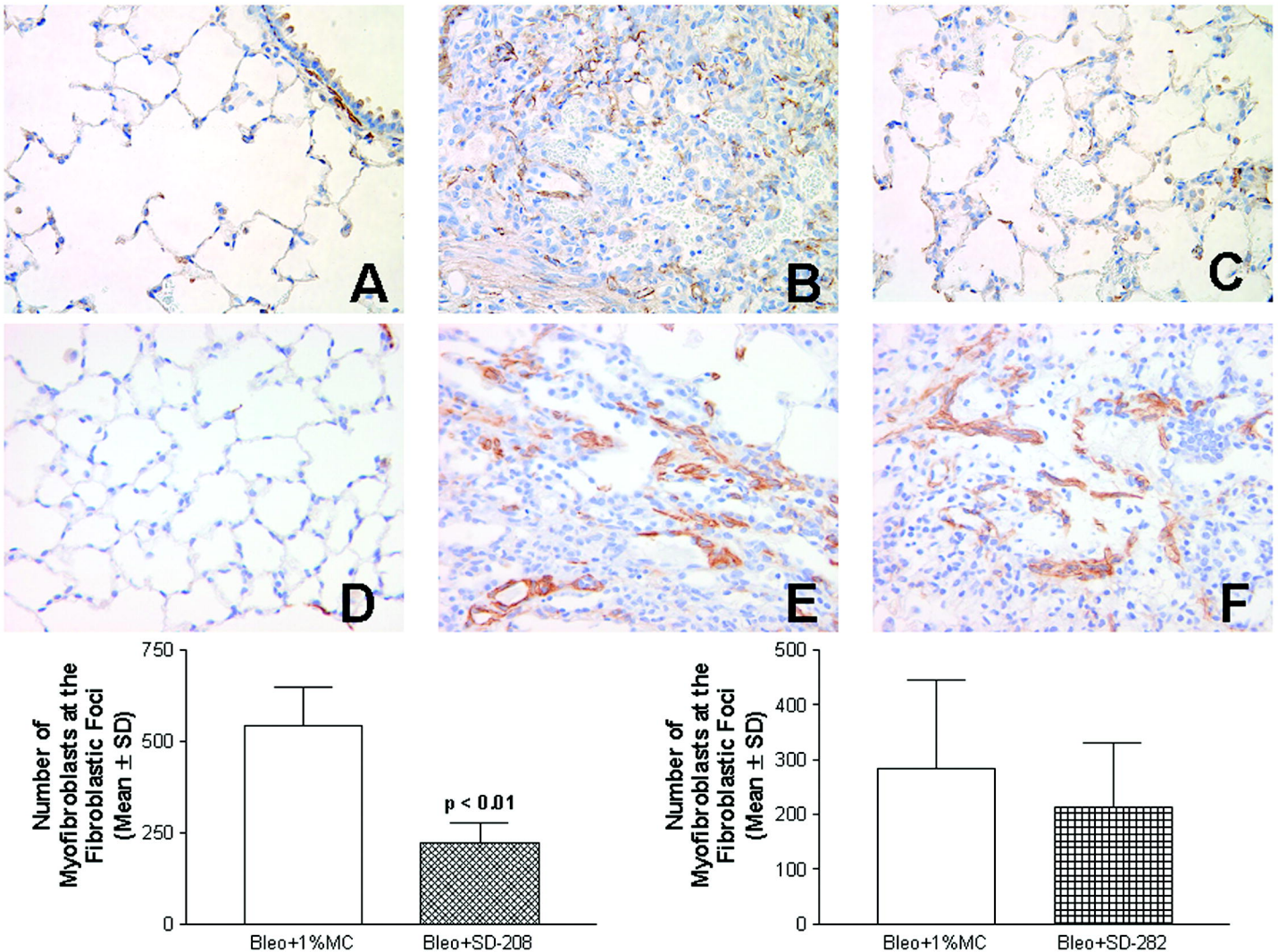
A
B
C
D
E
F
Number of Myofibroblasts at the Fibroblastic Foci (Mean ± SD)
750
500
250
0
p < 0.01
Bleo+1%MC
Bleo+SD-208
Number of Myofibroblasts at the Fibroblastic Foci (Mean ± SD)
500
400
300
200
100
0
Bleo+1%MC
Bleo+SD-282

Figure 7

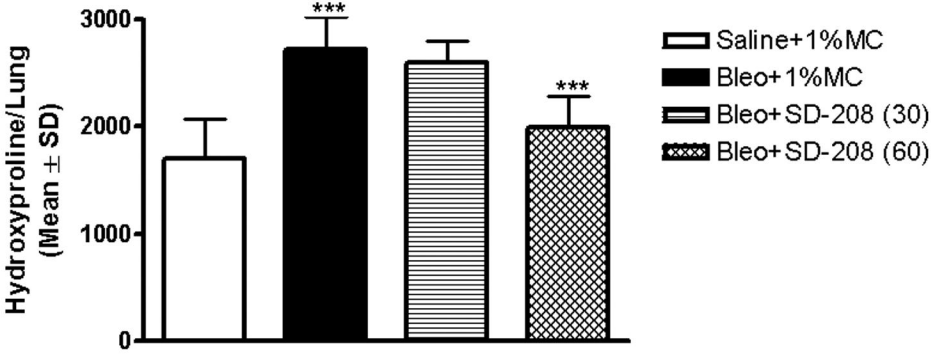
Hydroxyproline/Lung
(Mean ± SD)
3000
2000
1000
0
***
***
Saline+1%MC
Bleo+1%MC
Bleo+SD-208 (30)
Bleo+SD-208 (60)

Figure 8

A

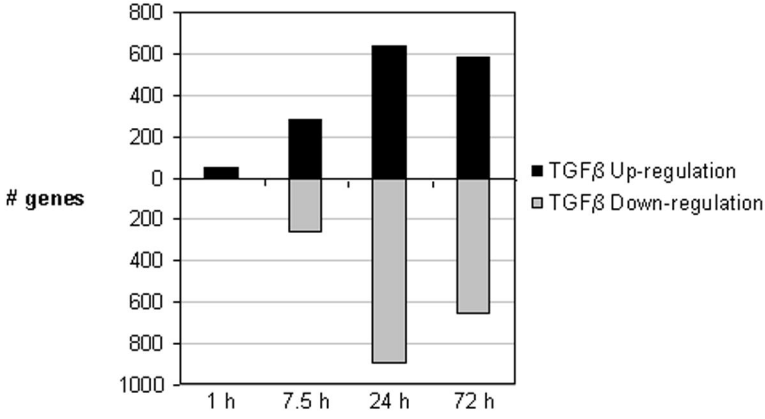
800
600
400
200
0
200
400
600
800
1000
genes
1 h
7.5 h
24 h
72 h
TGFβ Up-regulation
TGFβ Down-regulation

B

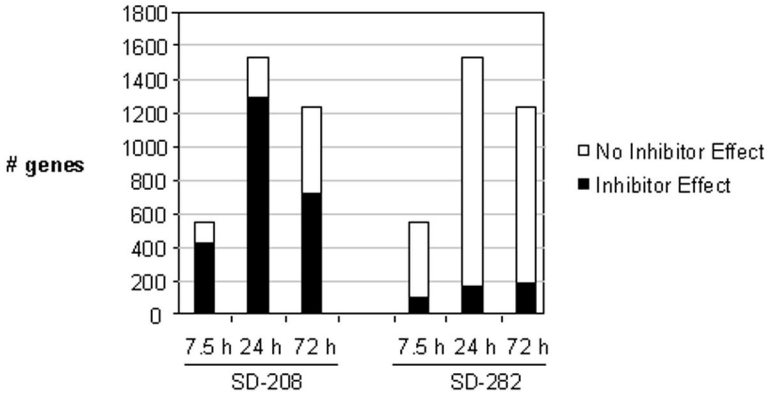
1800
1600
1400
1200
1000
800
600
400
200
0
genes
7.5 h 24 h 72 h
SD-208
7.5 h 24 h 72 h
SD-282
No Inhibitor Effect
Inhibitor Effect

C

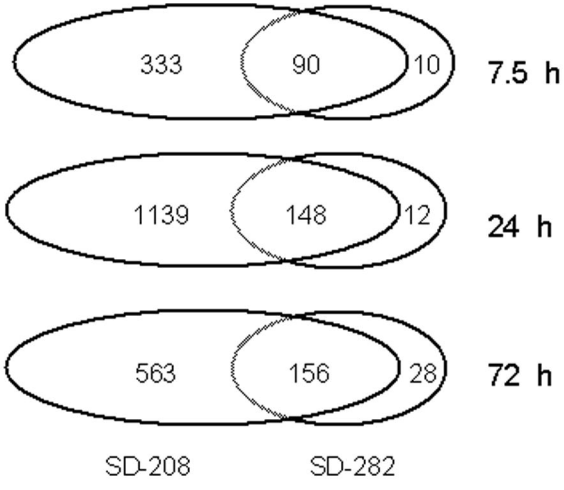
333
90
10
7.5 h
1139
148
12
24 h
563
156
28
72 h
SD-208
SD-282

Figure 9

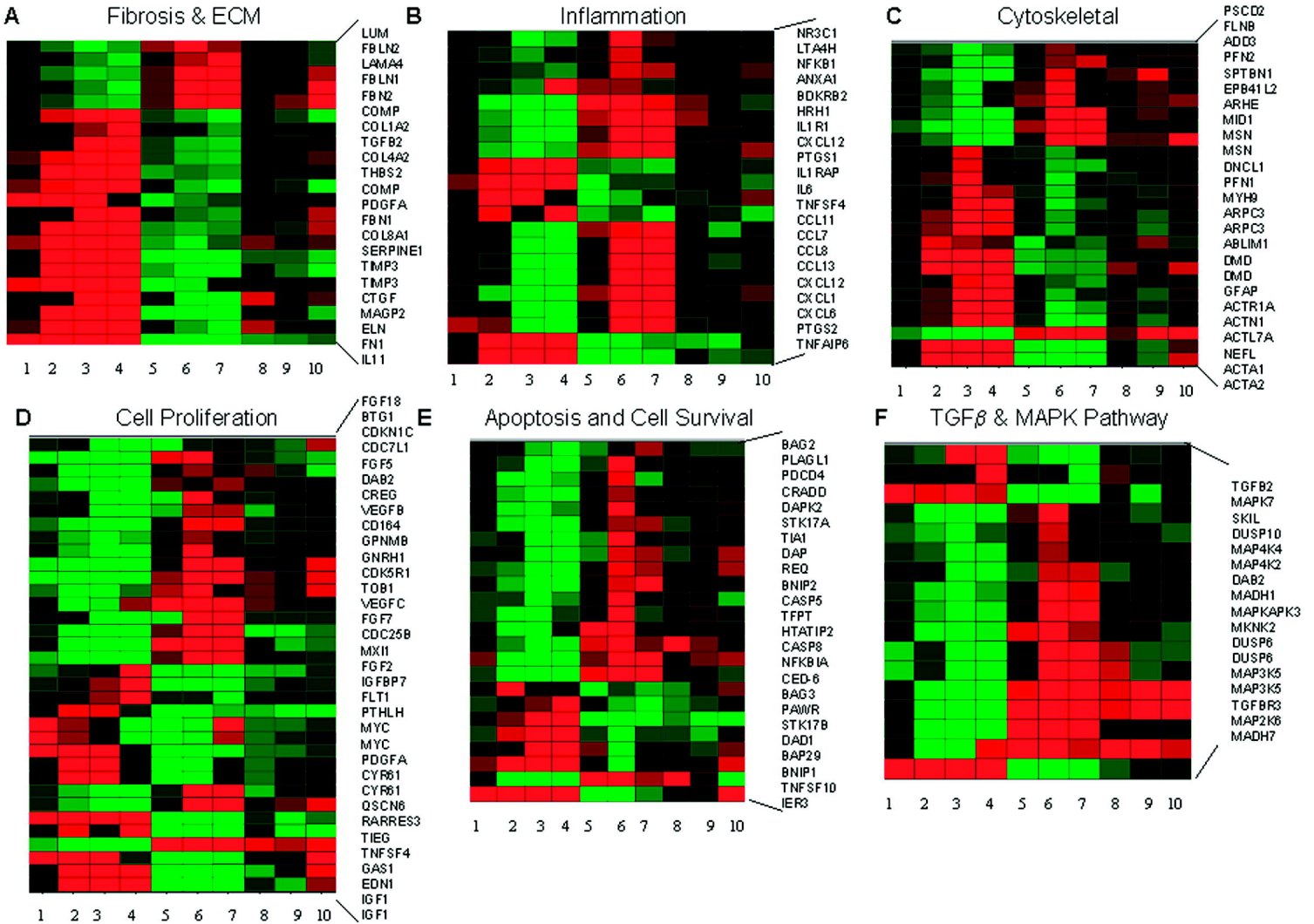
A
Fibrosis & ECM
LUM
FBLN2
LAMA4
FBLN1
FBN2
COMP
COL1A2
TGFB2
COL4A2
THBS2
COMP
PDGFA
FBN1
COL8A1
SERPINE1
TIMP3
TIMP3
CTGF
MAGP2
ELN
FN1
IL11
1 2 3 4 5 6 7 8 9 10
B
Inflammation
NR3C1
LTA4H
NFKB1
ANXA1
BDKRB2
HRH1
IL1R1
CXCL12
PTGS1
IL1RAP
IL6
TNFSF4
CCL11
CCL7
CCL8
CCL13
CXCL12
CXCL1
CXCL6
PTGS2
TNFAIP6
1 2 3 4 5 6 7 8 9 10
C
Cytoskeletal
PSCD2
FLNB
ADD3
PFN2
SPTBN1
EPB41L2
ARHE
MID1
MSN
MSN
DNCL1
PFN1
MYH9
ARPC3
ARPC3
ABLIM1
DMD
DMD
GFAP
ACTR1A
ACTN1
ACTL7A
NEFL
ACTA1
ACTA2
1 2 3 4 5 6 7 8 9 10
D
Cell Proliferation
FGF18
BTG1
CDKN1C
CDC7L1
FGF5
DAB2
CREG
VEGFB
CD164
GPNMB
GNRH1
CDK5R1
TOB1
VEGFC
FGF7
CDC25B
MXI1
FGF2
IGFBP7
FLT1
PTHLH
MYC
MYC
PDGFA
CYR61
CYR61
QSCN6
RARRES3
TIEG
TNFSF4
GAS1
EDN1
IGF1
IGF1
1 2 3 4 5 6 7 8 9 10
E
Apoptosis and Cell Survival
BAG2
PLAGL1
PDCD4
CRADD
DAPK2
STK17A
TIA1
DAP
REQ
BNIP2
CASP5
TFPT
HTATIP2
CASP8
NFKBIA
CED-6
BAG3
PAWR
STK17B
DAD1
BAP29
BNIP1
TNFSF10
IER3
1 2 3 4 5 6 7 8 9 10
F
TGFβ & MAPK Pathway
TGFB2
MAPK7
SKIL
DUSP10
MAP4K4
MAP4K2
DAB2
MADH1
MAPKAPK3
MKNK2
DUSP6
DUSP6
MAP3K5
MAP3K5
TGFBR3
MAP2K6
MADH7
1 2 3 4 5 6 7 8 9 10

Figure 10